

**N A S A   T E C H N I C A L  
R E P O R T**

**NASA TR R-164**

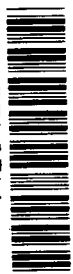


**NASA TR R-164**

*e.1*

LOAN COPY: RETU  
ATWL (WEL-4)  
KIRTLAND AFB, N

0068344



TECH LIBRARY KAFB, NM

**THEORETICAL STUDIES OF  
SUPERSONIC TWO-DIMENSIONAL AND  
AXISYMMETRIC NONEQUILIBRIUM FLOW,  
INCLUDING CALCULATIONS OF  
FLOW THROUGH A NOZZLE**

*by James J. Der*

*Ames Research Center  
Moffett Field, Calif.*



THEORETICAL STUDIES OF SUPERSONIC TWO-DIMENSIONAL  
AND AXISYMMETRIC NONEQUILIBRIUM FLOW, INCLUDING  
CALCULATIONS OF FLOW THROUGH A NOZZLE

By James J. Der

Ames Research Center  
Moffett Field, Calif.

and

Stanford University

NATIONAL AERONAUTICS AND SPACE ADMINISTRATION

---

For sale by the Office of Technical Services, Department of Commerce,  
Washington, D.C. 20230 -- Price \$1.50

# TABLE OF CONTENTS

	Page
LIST OF FIGURES . . . . .	ii
SUMMARY . . . . .	1
CHAPTER I - INTRODUCTION . . . . .	2
CHAPTER II - FLOW EQUATIONS . . . . .	5
CHAPTER III - SOME MATHEMATICAL PROPERTIES OF THE NONEQUILIBRIUM-FLOW EQUATIONS . . . . .	9
Direct Nozzle Problem . . . . .	17
Inverse Nozzle Problem . . . . .	17
CHAPTER IV - AXISYMMETRIC NONEQUILIBRIUM FLOW THROUGH A NOZZLE . . . . .	20
Gas Model . . . . .	20
Nozzle Model . . . . .	21
APPENDIX A - THERMODYNAMIC AND CHEMICAL-KINETIC PROPERTIES OF A SIMPLIFIED AIR MODEL . . . . .	36
APPENDIX B - PRINCIPAL SYMBOLS . . . . .	45
REFERENCES . . . . .	47

# LIST OF FIGURES

Figure	Page
III-1.- Characteristic lines for equations (III-1) . . . . .	12
III-2.- Domain of determinacy for equations (III-1a, b) . . . . .	13
III-3.- Domain of determinacy for equations (III-1c, d) . . . . .	14
III-4.- Data curves with overdeterminacy . . . . .	15
III-5.- Direct nozzle problem . . . . .	17
III-6.- Inverse nozzle problem . . . . .	18
IV-1.- Regions of flow in a typical high-speed nozzle . . . . .	20
IV-2.- Nozzle used in flow computations . . . . .	21
IV-3.- Characteristics net for nonequilibrium-flow computations . . . . .	23
IV-4.- Computation net for points on the nozzle center line, nozzle wall, and in the interior . . . . .	23
IV-5.- Degree of dissociation along the nozzle center line in the transition region for various degrees of nonequilibrium and various assumed nonequilibrium starting positions . . . . .	26
IV-6.- Characteristic reaction length in the transition region of the nozzle . . . . .	27
IV-7.- Degree of dissociation along the nozzle center line for various degrees of nonequilibrium . . . . .	28
IV-8.- Velocity along the nozzle center line for equilibrium and nonequilibrium flow . . . . .	29
IV-9.- Pressure along the nozzle center line at various degrees of nonequilibrium . . . . .	30
IV-10.- Temperature along the nozzle center line for various degrees of nonequilibrium . . . . .	31
IV-11.- Frozen Mach number along the nozzle center line for various degrees of nonequilibrium . . . . .	32
IV-12.- Variation of degree of dissociation across the nozzle-exit plane .	33
IV-13.- Velocity distribution across the nozzle-exit plane . . . . .	33

Figure	Page
IV-14.- Pressure distribution across the nozzle-exit plane . . . . .	34
IV-15.- Temperature distribution across the nozzle-exit plane . . . . .	34
IV-16.- Frozen Mach number distribution across the nozzle-exit plane . . .	34
A-1.- Equilibrium degree of dissociation versus temperature for pressure = 0.01, 1.0, and 100 atmospheres (simplified air model) . . . . .	40
A-2.- Equilibrium speed of sound versus temperature for pressure = 0.01, 1.0, and 100 atmospheres ( $a_{e0} = a_e$ at standard condition = $3.320 \times 10^4$ cm/sec) . . . . .	41
A-3.- Ratio of frozen to equilibrium sonic speed for the simplified air model and for pure oxygen . . . . .	42
A-4.- Normalized characteristic reaction length for the simplified air model and for pure oxygen . . . . .	43

NATIONAL AERONAUTICS AND SPACE ADMINISTRATION

---

TECHNICAL REPORT R-164

---

THEORETICAL STUDIES OF SUPERSONIC TWO-DIMENSIONAL AND  
AXISYMMETRIC NONEQUILIBRIUM FLOW, INCLUDING  
CALCULATIONS OF FLOW THROUGH A NOZZLE<sup>1</sup>

By James J. Der

SUMMARY

Chemical and vibrational nonequilibrium phenomena in steady two-dimensional and axisymmetric inviscid flow fields are studied by the analysis of flow past curved boundaries. The study consists of three parts: (1) formulation of the governing equations, (2) study of the general features of nonequilibrium flow by consideration of some mathematical properties of the nonlinear flow equations, and (3) analysis of axisymmetric flow of dissociated air through a nozzle by means of numerical computations.

In the formulation of the governing equations, possible alternative choices of the state variables to be used and their relative advantages are considered. The entropy is not found to be a convenient variable in nonequilibrium flow and is therefore not used. The system of nonequilibrium flow equations is two orders higher than the corresponding classical (equilibrium or frozen) system.

General features of the nonequilibrium flow are studied by examination of the mathematical properties of the nonlinear flow equations. In addition to the two differential compatibility equations along the Mach lines, as exist in classical supersonic flow, two more differential compatibility equations are necessary along the streamlines. The domain of determinacy of the nonequilibrium flow is the same as for classical flow, namely, the area bounded by the outermost Mach lines from a data curve. If a data curve is crossed more than once by any characteristic, the amount of data that can be prescribed is restricted. The implications of such restrictions in nozzle problems are discussed.

Finally, an axisymmetric nonequilibrium flow of air through a supersonic nozzle is analyzed by means of numerical computations. The coupling effects between nonuniformity (across a nozzle section) and nonequilibrium, not taken into account in the quasi-one-dimensional flow approximation, are revealed by the present analysis.

---

<sup>1</sup>This report is based on a dissertation submitted to the Department of Aeronautics and Astronautics, Stanford University, in partial fulfillment of the requirements for the Ph.D. degree. The work arose out of the author's participation in a graduate research seminar supported at Stanford University by a grant from the National Science Foundation.

## CHAPTER I

### INTRODUCTION

The present study is concerned with chemical and vibrational nonequilibrium<sup>2</sup> phenomena in two-dimensional and axisymmetric flow.

Studies of nonequilibrium flow have been concerned mainly with one-dimensional (refs. 1 through 3) and quasi-one-dimensional flow (refs. 4 through 11) and with two-dimensional and axisymmetric flow past bodies of simple shape (refs. 12 through 17).<sup>3</sup> A general formulation of the equations for nonequilibrium flow has been presented by Kirkwood and Wood (ref. 18) and by others (e.g., refs. 19 and 20). A method for the numerical computation of the quasi-one-dimensional flow of a general gas mixture has been formulated recently by Emanuel and Vincenti (ref. 8).

In the present work, the more general features of two-dimensional and axisymmetric nonequilibrium flow are studied by consideration of flow past curved boundaries. For simplicity the study is limited to the cases of supersonic flow with a single nonequilibrium process. Part of this objective was achieved in reference 21, which, however, was concerned only with linearized flow past a single wall.

In chapter II, the inviscid flow equations are given. Alternative forms of the governing equations and their possible advantages are discussed. The entropy, a convenient quantity in classical (frozen or equilibrium) gas dynamics, has no particular utility in the present analysis as a nonequilibrium variable. The constancy of a nonequilibrium parameter (other flow quantities varying) signifies the freezing of the corresponding nonequilibrium process. On the other hand, the entropy is constant along a streamline when the flow is either in an equilibrium or a frozen condition. The entropy is, therefore, not used in the formulation of the flow equations in the present work. The system of differential equations for nonequilibrium flows is seen to be two orders higher than the corresponding system for classical gas flows.

In chapter III, the general features of steady two-dimensional and axisymmetric nonequilibrium flow are studied by examination of some mathematical properties of the nonlinear flow equations. As in the case of classical gas dynamics, there are two differential compatibility relations along characteristics having the direction of the frozen Mach lines. In addition, however, there are two more differential compatibility relations necessary along the characteristic in the streamline direction. The domain of determinacy of the nonequilibrium flow is the same as that of the frozen flow, namely, the region bounded by the outermost frozen Mach lines from a data curve.

---

<sup>2</sup>When a nonequilibrium variable (such as a degree of dissociation) is in equilibrium with the other local thermodynamic state variables, the flow is said to be in equilibrium with respect to the corresponding nonequilibrium process; otherwise the flow is said to be in nonequilibrium condition. When a nonequilibrium variable becomes fixed, the flow is said to be frozen with respect to the corresponding nonequilibrium process.

<sup>3</sup>The references cited here constitute a representative rather than an exhaustive list of the numerous published works in this field.

For any system of hyperbolic differential equations, if a data curve is crossed by any characteristic line only once, full data can be posed on the data curve. If a data curve is crossed by any characteristic twice, then only partial initial values can be prescribed. For the system of equations used herein, the prescription of initial values of the pressure and stream angle will be restricted if the data curve is crossed twice by one of the frozen Mach lines (which is true also for the classical flow). On the other hand, prescription of the initial values of the velocity and the degree of dissociation will be restricted if the data curve is crossed twice by the streamlines. Nonequilibrium flow has more compatibility relations than the classical flow and hence has more restrictions on the prescription of initial values. These additional restrictions prevent us from prescribing a completely uniform exit flow in the inverse nozzle problem (i.e., computation of the contour of a nozzle for given initial, center line, and exit conditions).

Finally, a specific nonlinear, nonequilibrium flow problem is studied in chapter IV, where the dissociative nonequilibrium flow of air through a given nozzle is analyzed. The flow of real air is approximated by a flow of a mixture of dissociating oxygen and nondissociating nitrogen. The molecular vibration is assumed to be in equilibrium. The assumption of only a single nonequilibrium process simplifies the analysis considerably. For the present nozzle problem (temperature less than  $8000^{\circ}$  K, pressure less than 300 atmospheres), however, such approximation is valid since nitrogen dissociation is actually small. Four cases for the same reservoir conditions were computed numerically by means of an IBM 7090 digital computer. These include one equilibrium flow and three cases of nonequilibrium flow with varying degrees of nonequilibrium as dictated by the magnitude of the effective characteristic reaction length.

It is found that quasi-one-dimensional flow computations give qualitatively correct results. On the other hand, the coupling effects between nonuniformity (at a nozzle cross section) and nonequilibrium, not taken into account in quasi-one-dimensional flow, are revealed in the present analysis. At any cross section, the flow near the nozzle wall has traveled a longer distance than the flow near the nozzle center. Furthermore, the flow near the center line freezes sooner. Hence, near the center line the flow has higher values of the degree of dissociation. The nonuniformity at the nozzle exit worsens as the degree of nonequilibrium increases. The exit velocity changes only minutely and remains nearly uniform as the flow deviates from the equilibrium condition. Other flow variables, including pressure, temperature, and Mach number, change significantly both in magnitude and uniformity at the exit as the flow tends toward the frozen condition. In general, therefore, one can expect little effect on velocity due to nonequilibrium, but significant effects on Mach number and other variables. Also, since one cannot impose complete uniformity of all flow variables at the nozzle exit, prescribing uniform exit pressure in designing a nozzle would lead to more uniform flow over-all than prescribing uniform exit velocity.

The thermodynamic and chemical kinetic properties of the simplified air model used in the numerical analysis are listed in appendix A.

The author is indebted to Professor Walter G. Vincenti of Stanford University for his guidance throughout the course of the research and to Dr. Max. A. Heaslet of the National Aeronautics and Space Administration, Ames



Research Center, for his timely encouragement and assistance. Professor M. D. Van Dyke provided valuable criticism and encouragement. Finally, thanks are due to Professor I-Dee Chang for reading the manuscript and furnishing important criticism and assistance.

## CHAPTER II

### FLOW EQUATIONS

The governing equations of flow of a reacting gas in the absence of transport phenomena and body forces are the familiar conservation equations plus the equation of state and the rate equations. The rate equations, which are not used in classical (equilibrium or frozen) gas dynamics, are needed here because the more general state equation now contains additional nonequilibrium parameters, for example, the various molecular vibrational energies and the degree of dissociation and ionization of the various constituents. The equations for flow with  $n$  nonequilibrium parameters are, therefore (see e.g., ref. 22)

$$\text{Mass} \quad \frac{D\rho}{Dt} + \rho \operatorname{div} \vec{w} = 0 \quad (\text{II-1a})$$

$$\text{Momentum} \quad \rho \frac{D\vec{w}}{Dt} + \operatorname{grad} p = 0 \quad (\text{II-1b})$$

$$\text{Energy} \quad \rho \frac{Dh}{Dt} - \frac{Dp}{Dt} = 0 \quad (\text{II-1c})$$

$$\text{State} \quad h = h(p, \rho, q_1, \dots, q_n) \quad (\text{II-1d})$$

$$\text{Rate} \quad \frac{Dq_i}{Dt} = \omega_i(p, \rho, q_1, \dots, q_n) \quad i = 1, \dots, n \quad (\text{II-1e})$$

where  $D/Dt$  denotes the Eulerian derivative;  $\rho$ ,  $\vec{w}$ ,  $p$ ,  $h$  are the density, velocity, pressure, and enthalpy of the medium;  $q_i$  denotes the vibrational energy and/or degree of dissociation and ionization; and  $\omega_i$  gives the net rate of increase of  $q_i$  as a function of the local thermochemical state.

When the flowing gas is in equilibrium, the values of  $q_i$  are functions solely of the local pressure and density, hence the enthalpy becomes a function solely of  $p$  and  $\rho$ , that is

$$h_e = h[p, \rho, q_{ie}(p, \rho)] = h_e(p, \rho)$$

When the gas is in a frozen condition, each  $q_i$  has a certain fixed value, and  $h$  is again a function solely of  $p$  and  $\rho$ , that is,

$$h_f = h[p, \rho, q_i = \text{constant}] = h_f(p, \rho)$$

Note that a perfect gas has  $q_i = q_{ie}(p, \rho) = \text{constant}$ ; hence a perfect gas is, by definition, always in the frozen and equilibrium conditions simultaneously.

It is of interest to note the minimum number of first-order differential equations required to determine a flow field. We consider, for simplicity, steady two-dimensional and axisymmetric flow with only one mode of nonequilibrium. Since the state equation is not in differential form, it can be used to eliminate one dependent variable from the differential equations. We shall choose to eliminate  $\rho$ . This can be done by differentiating equation (II-1d) and using equations (II-1c) and (II-1e) together with the identity

$$a_F^2 \equiv \frac{h_p}{\rho^{-1} - h_p} \quad (\text{II-2})$$

for the frozen speed of sound (see appendix A), thus finding an expression for  $D\rho/Dt$  in terms of  $Dp/Dt$  and  $Dq_i/Dt$ . By substituting this expression into equation (II-1a), we obtain a modified mass equation. Furthermore, the energy equation can be modified by combining it with the momentum equation, yielding a form more convenient for our purpose. A complete set of differential equations governing nonequilibrium flow is thus obtained as

$$a_F^{-2} \frac{Dp}{Dt} + \rho \operatorname{div} \vec{w} - \sum_{i=1}^n \frac{h_{q_i}}{h_p} \omega_i = 0 \quad (\text{II-3a})$$

$$\rho \frac{D\vec{w}}{Dt} + \operatorname{grad} p = 0 \quad (\text{II-3b})$$

$$\rho \frac{D}{dt} \left( h + \frac{w^2}{2} \right) - \frac{\partial p}{\partial t} = 0 \quad (\text{II-3c})$$

$$\frac{Dq_i}{Dt} - \omega_i = 0 \quad (\text{II-3d})$$

The coefficients are related to the dependent variables,  $p$ ,  $\vec{w}$ ,  $h$ ,  $q_i$ .

For steady flow, equation (II-3c) can be integrated immediately, yielding an algebraic relation stating that the sum  $h + w^2/2$  is constant along each streamline. We further restrict our study to two-dimensional axisymmetric flow, with only one nonequilibrium parameter. Equations (II-3) then become, in intrinsic coordinates,

$$M_F^2 \frac{\partial p}{\partial s} + \rho w \left( \frac{\partial w}{\partial s} + w \frac{\partial \theta}{\partial n} \right) + \left( \frac{v-1}{r} \rho w^2 \sin \theta - \frac{h_q}{h_p} w w \right) = 0 \quad (\text{II-4a})$$

$$\rho w \frac{\partial w}{\partial s} + \frac{\partial p}{\partial s} = 0 \quad (\text{II-4b})$$

$$\rho w^2 \frac{\partial \theta}{\partial s} + \frac{\partial p}{\partial n} = 0 \quad (\text{II-4c})$$

$$\frac{\partial q}{\partial s} - \frac{\omega}{w} = 0 \quad (\text{II-4d})$$

where  $M_F \equiv w/a_F$ ;  $s$  and  $n$  are the streamwise and normal coordinates;  $\theta$  is the streamline angle;  $v$  is 1 for planar flow and 2 for axisymmetric flow; and  $r$  is the radial distance from the center line of axial symmetry.

The minimum number of first-order differential equations governing a steady, nonequilibrium, two-dimensional or axisymmetric flow is thus seen to be four.

In the classical limits of either equilibrium or frozen flow, two more differential equations can be eliminated. This can be done by introducing the specific entropy  $S$ , which is related to  $\omega_i$  by the relation

$$T \frac{DS}{Dt} = \sum_{i=1}^n z_i \omega_i \quad (\text{II-5})$$

where the  $z_i$  are related to the chemical potential and the vibrational energies (see, e.g., ref. 18). (The specific entropy is denoted here by  $S$  to avoid confusion with the streamwise coordinate  $s$ .) The rate of change of entropy  $DS/Dt$  is zero when the flow is frozen ( $\omega_i = 0$ ) or in equilibrium ( $\sum z_i \omega_i = 0$ ). Furthermore, since the state of the medium in either limit is determined by only two thermodynamic variables, we can take one of these to be the entropy, which is, from equation (II-5), constant along streamlines. The two relations,  $h = h(p, S)$  and  $S = \text{constant}$  along a streamline, can then be used to replace two of the differential equations, equations (II-4b) and (II-4d). In the frozen and equilibrium limits, therefore, the order of the system of flow equations is 2. This is true regardless of whether the flow is rotational or irrotational.

The governing differential flow equations can be written in various alternative forms. For special purposes a particular form of the equations may have advantages over the others. The differences among various forms of the equations arise mostly from the choice of the state equation. Choice of equation (II-1d) is natural because it relates  $h$ , which arises naturally in the energy equation for fluid flow, to  $p$  and  $\rho$ , which appear in the mass and momentum equations. Equations (II-1) are convenient for analytical purposes.

A perhaps more familiar way of expressing the state relationship is to relate  $h$ ,  $p$ , and  $\rho$  by means of the two equations

$$h = h(\rho, T, q_i) \quad (\text{II-6a})$$

$$p = p(\rho, T, q_i) \quad (\text{II-6b})$$

with the temperature  $T$  as a parametric quantity. These two equations are called, respectively, the caloric and thermal equations of state. For numerical computations, equations (II-6) are often convenient to use because the temperature usually appears as a natural variable in the thermodynamic and kinetic relations for real gases, such as air (see appendix A).

The entropy, useful in classical gas dynamics, especially when the flow is homoentropic, is not nearly so convenient in nonequilibrium flow since here entropy is not constant along streamlines. On the other hand, the constancy of the  $q_1$  (with other flow quantities varying) signifies that the flow is in the frozen condition. Furthermore, the derivative of entropy in equation (II-5) contains  $z_1$  and  $\omega_1$ , and in some conditions both of these become indeterminate. The use of entropy, therefore, may affect the stability of the numerical integration process. If one needs to examine the variation of entropy, it is preferable to compute it from equation (II-5) after the flow has been found in terms of other variables.

## CHAPTER III

### SOME MATHEMATICAL PROPERTIES OF THE NONEQUILIBRIUM-FLOW EQUATIONS

We now consider the application of the flow equations (eqs. II-4) developed in the last chapter to problems of fluid flow in nonequilibrium condition. These equations are quasi-linear<sup>4</sup> with complicated coefficients. Practical solutions to such equations can be obtained, except in special cases, only by numerical methods. We can study some of the general characteristics of nonequilibrium flow, however, by examining a few mathematical properties of the nonequilibrium flow equations and comparing them with those of the classical flow equations.

For simplicity we restrict our study to cases of only one nonequilibrium process since the extension to multiprocess cases introduces no additional difficulties. Again, we study only steady two-dimensional or axisymmetric flow. Supersonic flow will be dealt with mostly, although some of the discussion applies to more general speed regimes. After some general discussion of the mathematical properties, we apply the results to nozzle problems with regard to the posing of initial and boundary values. Strong discontinuities such as shock waves and slip lines will not be considered.

Some mathematical questions of special interest are the following:

1. What is the minimum number of dependent variables that determine the flow field?
2. What are the characteristics?
3. What must be continuous, and what can be discontinuous, across the characteristics?
4. What is the domain of determinacy?
5. How can the initial values be prescribed?
6. What can be said about the existence and uniqueness of the solution?

We may try to study these questions in terms of either a single  $n$ th order differential equation or a system of  $n$  first-order equations. We choose the latter because, as pointed out by Courant (ref. 23):

1. A higher order differential equation can be rewritten as a system of first-order equations, but the reverse is not true in general.
2. It is clearer to speak of the "fundamental" flow quantities, such as velocity and pressure, than of some relatively remote function of the flow variables, such as the stream function.

---

<sup>4</sup>A quasi-linear differential equation is linear in its highest derivatives.

3. The gas-dynamic equations can be written readily as a system of first-order equations.

The minimum number of dependent variables that determine the flow field is, of course, the same as the minimum number of differential equations. As shown in chapter II, the minimum number of differential equations in the present case is four. The dependent variables selected are  $p$ ,  $\theta$ ,  $w$ , and  $q$ , but any appropriate function of these variables could also be used.

The characteristics of a system of differential equations can be defined in various ways. The definition used by von Mises (ref. 24) is as follows:

"Curves along which analytically different solutions of a differential equation or a system of such equations can be patched together are called characteristics of the equation or system."

Here patching means the solutions on both sides of the curve are equal. Characteristics are thus curves across which the solutions themselves must be continuous but the normal derivatives of any order can be discontinuous. This type of discontinuity is called a weak discontinuity.

An equivalent definition of the characteristics is that along a characteristic certain partial derivatives of the equations group together in such a manner that they form a differential equation containing only ordinary derivatives in the direction of the characteristic. The characteristics and compatibility relations for the nonequilibrium-flow equations can readily be obtained by using this last definition. The direction along which an ordinary differential equation is formed is then the direction of a characteristic. The ordinary differential equation itself provides the compatibility relation corresponding to this characteristic. The compatibility relations are, in fact, the original differential equations written in characteristic form. The order of the system remains unchanged. Thus, in the present case we look for four compatibility relations.

Equations (II-4b) and (II-4d) are already in characteristic form along the streamlines. After elimination of the derivative of  $w$  by means of equation (II-4b), the partial derivatives in equations (II-4a) and (II-4c) can be grouped in such a manner that these two equations form a set of two ordinary differential equations in terms of  $p$  and  $\theta$  along the two frozen Mach lines. Briefly, these equations can be obtained as follows: If we eliminate  $\partial w / \partial s$  by the use of equation (II-4b), equation (II-4a) becomes

$$(M_f^2 - 1) \frac{\partial p}{\partial s} + \rho w^2 \frac{\partial \theta}{\partial n} + \left( \frac{v - 1}{r} \rho w^2 \sin \theta - \frac{h_g}{h_p} w w \right) = 0$$

The total differentials of  $p$  and  $\theta$  in the  $l$  direction (defined by the slope  $dn/ds$  of  $l$ ) can be written as

$$dp = \frac{\partial p}{\partial s} ds + \frac{\partial p}{\partial n} dn$$

and

$$d\theta = \frac{\partial \theta}{\partial s} ds + \frac{\partial \theta}{\partial n} dn$$

Solving these equations for  $\partial p / \partial s$  and  $\partial \theta / \partial n$  in terms of the directional derivatives  $dp/ds$  and  $d\theta/dn$ , substituting into the foregoing equation, and noting that  $\rho w^2 \partial \theta / \partial s = -\partial p / \partial n$  (from eq. (II-4c)), we have

$$\beta_f^2 \frac{dp}{ds} + \rho w^2 \frac{d\theta}{dn} + \left( \frac{ds}{dn} - \beta_f^2 \frac{dn}{ds} \right) \frac{\partial p}{\partial n} + \left( \frac{v-1}{r} \rho w^2 \sin \theta - \frac{h_q}{h_p} w \right) = 0$$

If we choose  $dn/ds = \pm 1/\beta_f$ , then the term containing the partial derivative  $\partial p / \partial n$  vanishes, and we thus obtain two ordinary differential equations along  $l_1$  and  $l_2$ , that is, along

$$\left( \frac{dn}{ds} \right)_{l_1} = \frac{1}{\beta_f} \quad \text{or} \quad \frac{dl_1}{ds} = \frac{M_f}{\beta_f}$$

and

$$\left( \frac{dn}{ds} \right)_{l_2} = -\frac{1}{\beta_f} \quad \text{or} \quad \frac{dl_2}{ds} = -\frac{M_f}{\beta_f}$$

In terms of  $l_1, l_2$ , therefore, we have

$$\beta_f dp \pm \rho w^2 d\theta + \left( \frac{v-1}{M_f r} \rho w^2 \sin \theta - \frac{h_q}{M_f h_p} w \right) dl_{1,2} = 0 \quad (\text{III-1a,b})$$

$$\text{along} \quad \frac{dr}{dx} = \tan(\theta \pm \mu)$$

and

$$\left. \begin{aligned} \rho w dw + dp &= 0 \\ w dq - \omega ds &= 0 \end{aligned} \right\} \text{along} \quad \frac{dr}{dx} = \tan \theta \quad \begin{aligned} &(\text{III-1c}) \\ &(\text{III-1d}) \end{aligned}$$



where  $\beta_F \equiv \sqrt{M_F^2 - 1}$ ;  $l_1$  and  $l_2$  are the distances along the left-running and right-running Mach lines, respectively (fig. III-1);  $r$  is the radial distance from the line of symmetry, which is also the  $x$ -axis; and  $\mu$  is the Mach angle, related to  $M_F$  by the relation  $\mu = \sin^{-1}(1/M_F)$ .

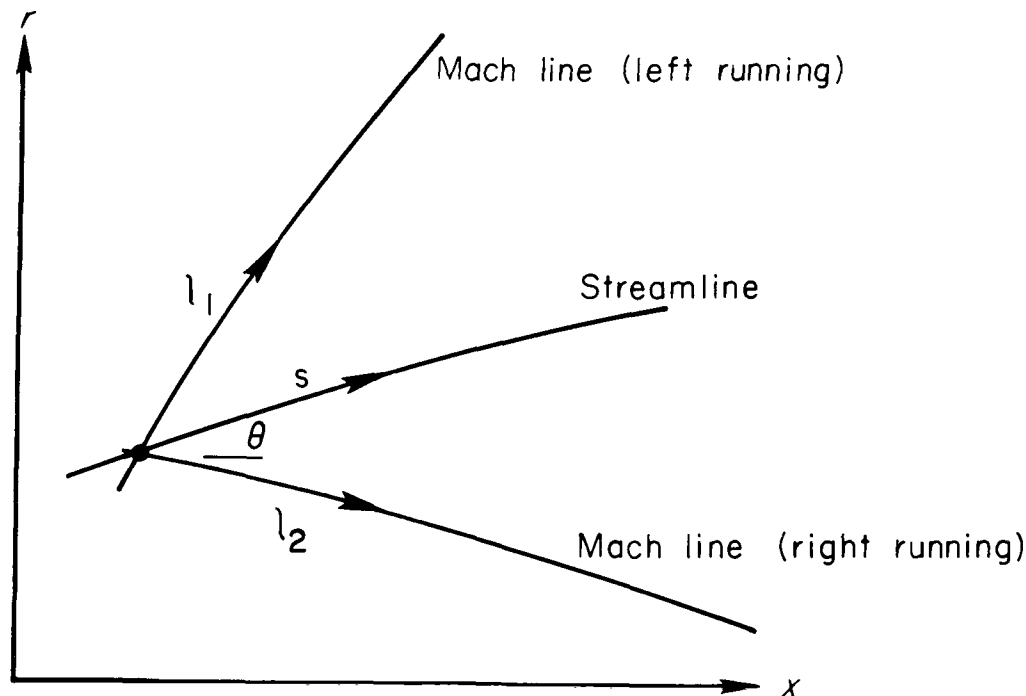


Figure III-1.- Characteristic lines for equations (III-1).

There are other, alternative forms of the compatibility relations. They can be obtained by the use of different variables. In general, the number of compatibility relations needed is the same as the number of original differential equations. Normally, there are two along the slant characteristics, or Mach lines, and the remainder along the streamlines. In selecting a particular set of compatibility relations, or variables, one should take into account the manner in which the problem is prescribed.

We can now deduce from equations (III-1) the answers to the questions posed earlier. First of all,  $p$ ,  $w$ ,  $\theta$ ,  $q$  constitute the solution to the system of equations, and hence these flow quantities must be continuous everywhere in the domain of weak discontinuities (i.e., in a flow field free of shock waves and slip lines). Equation (III-1a) is the characteristic equation for  $p$  and  $\theta$  along the left-running Mach line, whereas equation (III-1b) is the characteristic equation for  $p$  and  $\theta$  along the right-running Mach line. Across any Mach line, therefore, the normal derivatives of  $p$  and  $\theta$  can be discontinuous. Equation (III-1c), on the other hand, is the characteristic equation for  $p$  and  $w$  along the streamlines. It follows that the normal derivatives of  $p$  and  $w$  can be discontinuous across a streamline. Similarly, due to equation (III-1d), the normal derivative of  $q$  can be discontinuous across a streamline.

Note that, alternatively,  $p$  instead of  $w$  could have been eliminated in forming equations (III-1a,b). The variable  $w$ , therefore, can have a weak discontinuity (normal derivative discontinuous) across the Mach lines also. The quantity  $\theta$ , however, cannot have a weak discontinuity across a streamline. This can be deduced by the use of equation (II-4a) as follows: Since all of the coefficients and, in general,  $\partial p / \partial s$  and  $\partial w / \partial s$  are continuous across the streamline, it follows that  $\partial \theta / \partial n$  must be continuous across a streamline. Similarly, that the quantity  $q$  cannot have a weak discontinuity across a Mach line can be deduced from the fact that  $\partial q / \partial s$  is always continuous (since  $w$  is always continuous) and  $\partial q / \partial l_{1,2}$  are in general continuous (since  $q$  is in general continuous). Summarizing:

$p, w, \theta$  can have weak discontinuities across a Mach line, while  $p, w, q$  can have weak discontinuities across a streamline. Weak discontinuities cannot occur in  $q$  across Mach lines nor in  $\theta$  across streamlines. The actual occurrence of any such discontinuity, of course, is dependent on the initial conditions.

From the point of view of analysis, the characteristic equations have two properties of significance. One is that they are ordinary differential equations along the characteristic lines, and hence enable us to use a relatively well developed numerical integration scheme. (This scheme is discussed in chapter IV.) The other is that the variation of the flow quantities along the characteristics cannot be arbitrary but is restricted by the relationships fixed by the characteristic equations. These restrictions limit the freedom with which initial values of  $p, w, \theta, q$  can be prescribed. The nonequilibrium flow requires a larger number of characteristic equations than the classical flow and hence has more restrictions. We can more readily visualize the problem of posing the initial conditions after the domain of determinacy is discussed.

The theory of characteristics has been studied extensively for linear equations. The results of these studies can be extended by successive approximations to quasi-linear equations. Here, we are specifically interested in the domain of determinacy. Consider figure III-2 where initial data are prescribed

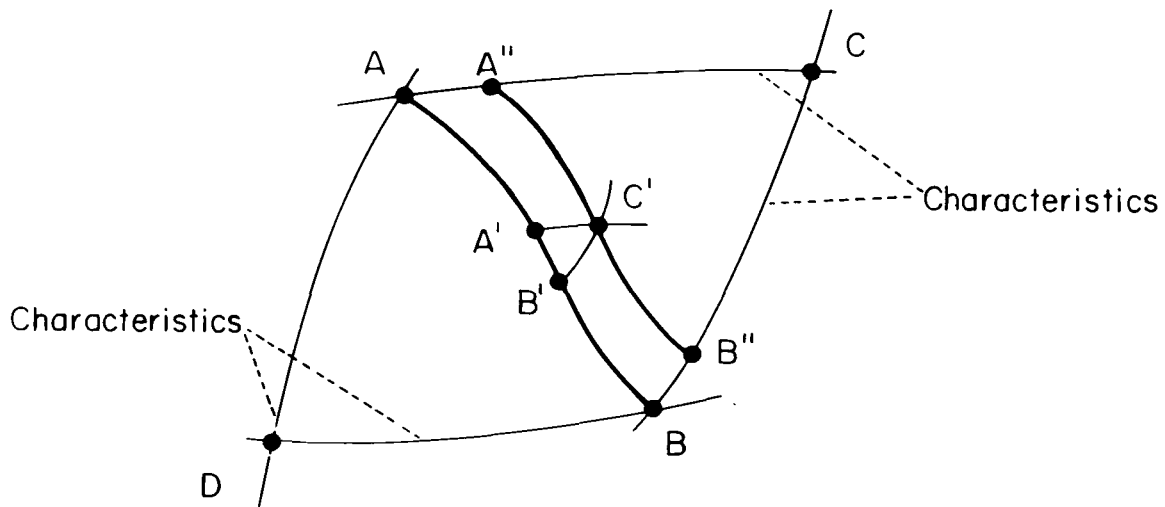


Figure III-2.- Domain of determinacy for equations (III-1a, b).

on the data curve AB. By data curve we mean a segment of a curve along which the initial values of the dependent variables of a system of differential equations are prescribed. If the initial values of all the dependent variables of the system of equations are prescribed, this segment is said to have full data, otherwise the data curve is said to have partial data. A data curve may or may not constitute the data curve of the entire problem (flow field in the present case); and the system of equations may be either the complete system, that is, all of equations (III-1), or a subsystem of it, for example, equations (III-1a,b).

If the subsystem of equations (III-1a,b) were linear, the domain of determinacy, with full data of this subsystem prescribed on AB, is the area ACBD bounded by the outermost slant characteristics (frozen Mach lines) AC, BC, AD, and BD.

For our equation, which is quasi-linear instead of strictly linear, we can apply the iterative procedure of Schauder (ref. 23, p. 476) to compute the flow quantities to any desired accuracy in the small region  $A'B'C'$ , where  $A'C'$  and  $B'C'$  are characteristics. By continuing the process over the full length of AB, we can determine the flow quantities in the region  $AA''B''B$  in the near neighborhood of AB. We thus obtain a new data line  $A''B''$ . By continuing the process toward C and also toward D, we can determine the entire region ACBD bounded by the outermost characteristics. For the nonlinear equations, of course, the location of the characteristics is not known in advance, but must be computed successively. According to reference 23 (p. 466), the above iterative solution converges and is unique, and the solution can be extended to a finite domain containing weak discontinuities. Hence, the solution to the quasi-linear equations exists and is unique in domain ACBD.

In our system of equations, we have not only slant characteristics, that is, the Mach lines, but also the streamwise characteristics defined by the streamlines. If equations (III-1c,d) were linear, the domain of determinacy of each of these subsystems (eq. III-1c, eq. III-1d) would be an infinite strip bounded on the sides by the outermost streamlines passing through the initial data line AB (fig. III-3).

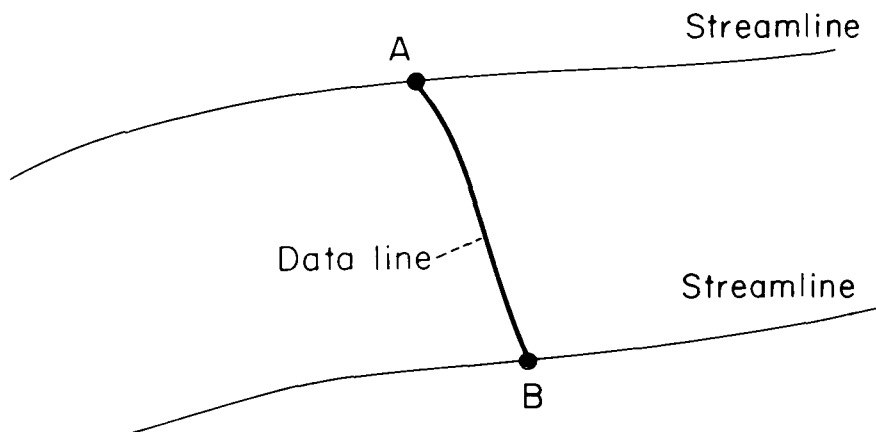


Figure III-3.- Domain of determinacy for equations (III-1c, d).

All of the subsystems (eqs. III-1a,b; III-1c; III-1d) are, of course, coupled. For example, the coefficients for equations (III-1a,b) are functions not only of  $p$  and  $\theta$  but also of  $w$  and  $q$ . Equation (III-1c) likewise has a coefficient that is a function of  $p$ ,  $w$ , and  $q$ , and, in addition, the quantity  $p$  appearing in the differential is to be found from the subsystem equations (III-1a,b). The domain of determinacy of the complete system of equations (III-1) is, therefore, the common domain of determinacy of all the subsystems. Thus, the domain of determinacy of the complete system is the same as that for subsystem equations (III-1a,b), that is, the region bounded by the outermost slant characteristics.

In posing the initial conditions we must take care that no region is overdetermined. In specifying the initial values of  $p$  and  $\theta$ , for example, we must inquire whether the data curve is crossed more than once by any Mach line (since the Mach lines are the characteristics for the subsystem equations (III-1a,b)). To see this we refer to figure III-4. The segments  $AB$ ,  $BB_1$ , and  $BB_2$  are data curves. If the initial values of  $p$  and  $\theta$  (as well as  $w$  and  $q$ ) are prescribed on  $AB$ , then, since  $BB_1$  lies inside the domain of determinacy of  $AB$ , the values of  $p$  and  $\theta$  on  $BB_1$  are determined. Hence, neither  $p$  nor  $\theta$  can be prescribed on  $BB_1$ . In other words, if a curve (e.g.,  $ABB_1$ ) is

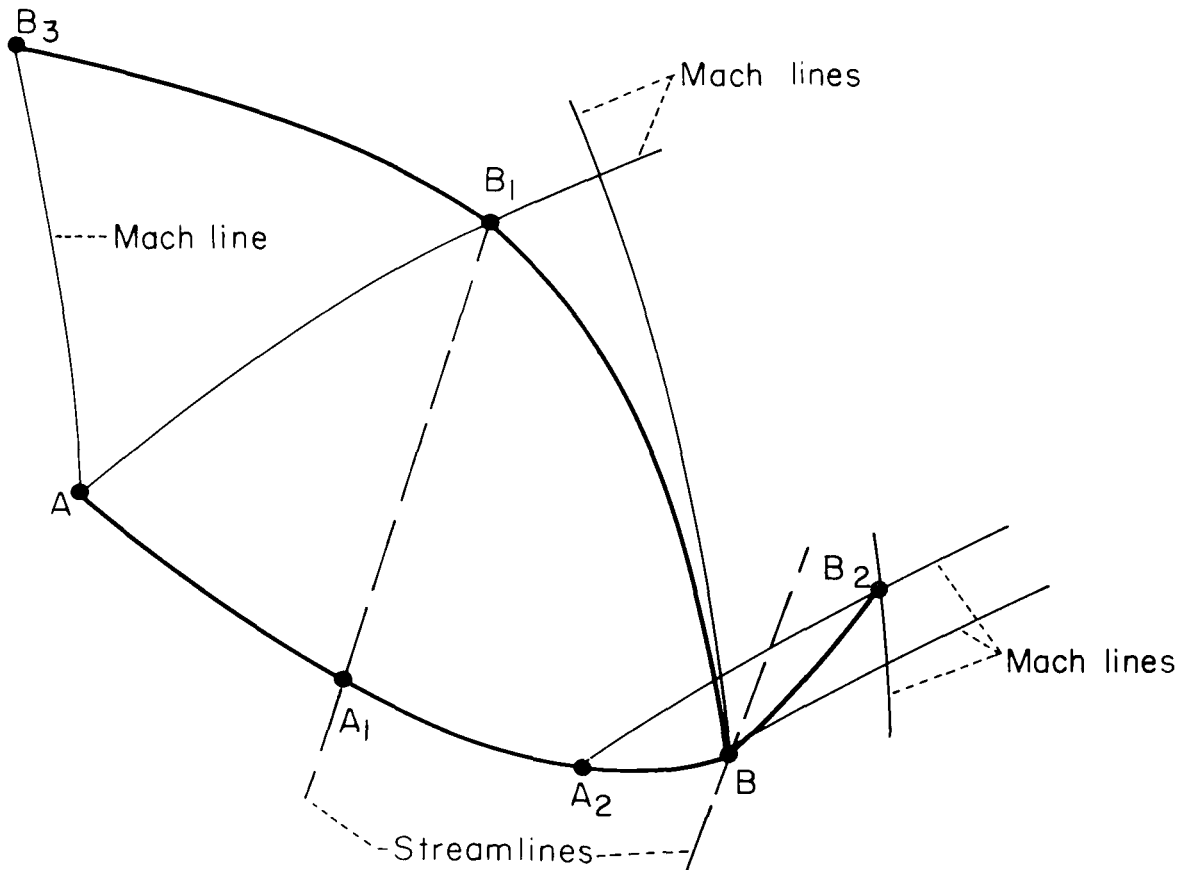


Figure III-4.- Data curves with overdeterminacy.

crossed twice by both the left-running and right-running Mach lines, then one segment of it ( $BB_1$ ) lies inside the domain of determinacy (for  $AB$ ) of the subsystem equations (III-1a,b). Consequently, the full data of this subsystem (values of  $p$  and  $\theta$ ) can be prescribed only on one segment ( $AB$ ). Posing partial data on both segments ( $AB$  and  $BB_1$ ) is possible, however. For example, if  $p$  only is prescribed on  $AB$  and  $\theta$  only is prescribed on  $BB_1$  (and also on  $B_1B_3$ ), then,  $p$  for  $BB_1$  and  $\theta$  for  $AB$  are determined by equations (III-1a,b).

Another situation that can arise is illustrated as follows: The curve  $A_2BB_2$  is crossed twice by only one of the two families of Mach lines. The data prescription on such a curve is less restrictive than that on a curve of the type  $ABB_1$ . If full data for the subsystem equations (III-1a,b) (both  $p$  and  $\theta$ ) are prescribed on  $A_2B$ , then the values of  $p$  and  $\theta$  on  $BB_2$  are related by equation (III-1b). Consequently, either  $p$  or  $\theta$ , but not both, can be prescribed on  $BB_2$ .

In posing data for  $w$  and  $q$ , we need to note whether the data curve for  $w$  or  $q$  is crossed more than once by a streamline. In figure III-4,  $A_1BB_1$  is crossed twice by the streamlines. If the initial value of  $w$  is prescribed on  $A_1B$  then the value of  $w$  on  $BB_1$  is related to that on  $A_1B$  by equation (III-1c). The initial value of  $w$  (and similarly  $q$ ) can be prescribed on either  $A_1B$  or  $BB_1$  but not on both.

The foregoing are the restrictions imposed by the characteristic relation as mentioned earlier in this chapter. We can summarize these restrictions as follows (referring to fig. III-4):

I. If a data line is crossed twice by

A. both families of the Mach lines (say first segment  $AB$ , then segment  $BB_1$ ), then the initial value of  $p$  and  $\theta$  can be posed in one of two ways:

1. Prescribe  $p$  and  $\theta$  on  $AB$  or  $BB_1$  only.
2. Prescribe  $p$  on  $AB$  and  $\theta$  on  $BB_1$  or vice versa.

B. only one family of Mach lines, then both  $p$  and  $\theta$  can be prescribed on one of the segments and either  $p$  or  $\theta$  on the other segment.

II. If a data line is crossed by the streamlines twice (say first  $A_1B$ , then  $BB_1$ ), then  $w$  can be prescribed on one of the two segments only. The same is true for  $q$ .

We illustrate these points by the following two examples.

### Direct Nozzle Problem

In the direct nozzle problem, for which calculations are made in the next chapter, initial data can be prescribed on AB (fig. III-5). For our system,

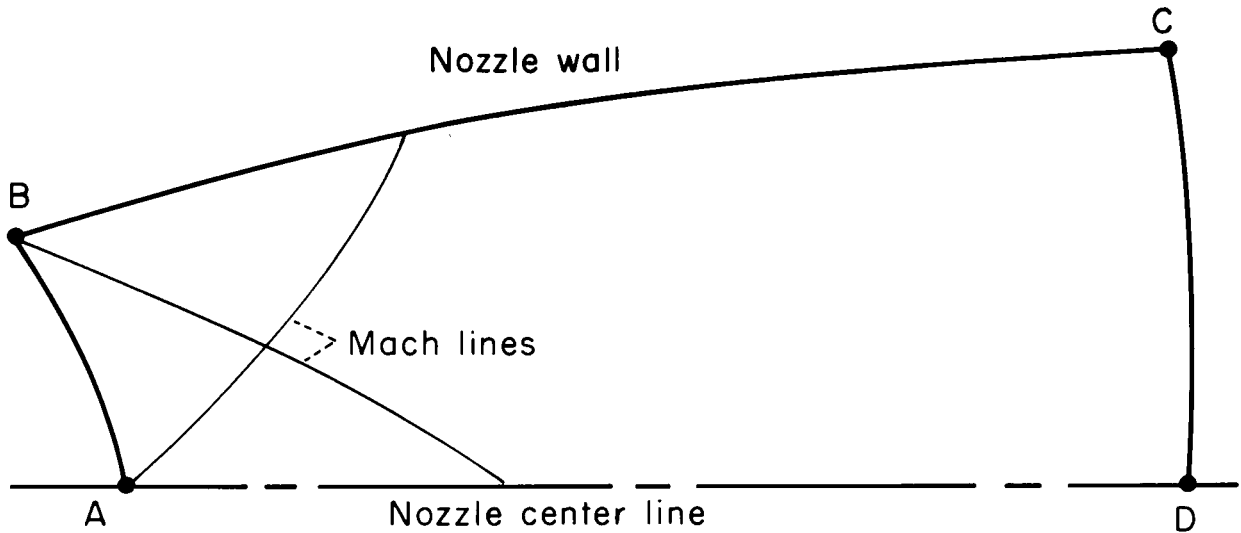


Figure III-5.- Direct nozzle problem.

the data that can be prescribed on this line are  $p$ ,  $w$ ,  $\theta$ ,  $q$ . The values of  $\theta$  are also prescribed on AD where  $\theta = 0$  and BC where  $\theta = \theta(x)$ . Curve BAD is crossed twice by only the right-running Mach lines and therefore  $p$  and  $\theta$  can be prescribed on AB and  $\theta$  alone can be prescribed on AD. Similarly,  $\theta$  alone can be prescribed on BC. Curve ABCD is crossed by the streamlines twice; hence  $w$  and  $q$  can be prescribed either on AB or CD, but not both.

The posing of initial values in the direct nozzle problem is thus straightforward even for nonequilibrium flow. The inverse nozzle problem, on the other hand, is more deceptive.

### Inverse Nozzle Problem

In the inverse nozzle problem, usually the initial values are given in the throat region; certain desired exit and center-line conditions are also prescribed. The problem is to find the nozzle contour that gives these conditions.

Suppose we prescribe the initial values of  $p, \theta, w, q$  on  $AB$  (fig. III-6) which is a curve crossed only once by any characteristic. The value of  $\theta = 0$  is

Figure III-6.- Inverse nozzle problem.

In nozzle design it is usually desired that the flow at the exit be uniform. If  $CD$  in figure III-6 is perpendicular to the nozzle center line, we can let  $CD$  represent the exit plane. To prescribe that the flow be parallel on the exit plane, we let  $\theta = 0$  on  $CD$ . To have completely uniform flow we would further require that  $p, w, q$  be constant along  $CD$ . However, as previously concluded, we can prescribe only  $p$  and  $\theta$  on  $CD$ . We can therefore have only a parallel flow on the exit plane with  $p$  uniform, with no assurance that  $w$  and  $q$  will also be uniform. Alternatively, we could, of course, prescribe  $w$  and  $q$  as uniform on  $CD$  instead of having given values on  $AB$ . Unfortunately, however, prescribing  $w$  and  $q$  on  $CD$  may dictate unrealistic conditions at the entrance  $AB$  of the nozzle (the same is true, of course, for the direct nozzle problem).

For the design of a nozzle with the flow either frozen or in equilibrium, the above dilemma does not occur because in these cases the specification that  $\theta$  be zero and  $p$  uniform on  $CD$  leads automatically to uniformity of all other flow quantities on  $CD$ .

Finally, we recall that  $w$  can exchange roles with  $p$  in the formulation of the characteristic equations. We can therefore alternatively prescribe  $w$  instead of  $p$  to be uniform on  $CD$  ( $q$  being unspecified in both cases). The results of chapter IV will show, however, that  $w$  is nearly uniform anyway for a reasonably shaped nozzle. As a practical matter, therefore, the prescription of uniform  $p$  rather than  $w$  on the exit is to be preferred.



## CHAPTER IV

### AXISYMMETRIC NONEQUILIBRIUM FLOW THROUGH A NOZZLE

We now study the flow of air through a high-speed nozzle where the air is out of chemical equilibrium. Specifically, we study the physical phenomena associated with dissociation nonequilibrium when the flow is not uniform across each section of the nozzle. We can thus examine the interrelated effects of nonequilibrium and nonuniformity.

A typical nozzle is sketched in figure IV-1. To have significant effects of nonequilibrium, the air in the reservoir should be substantially dissociated, which means that the reservoir temperature must be high. This is usually the condition in a shock tunnel or spark-heated tunnel.

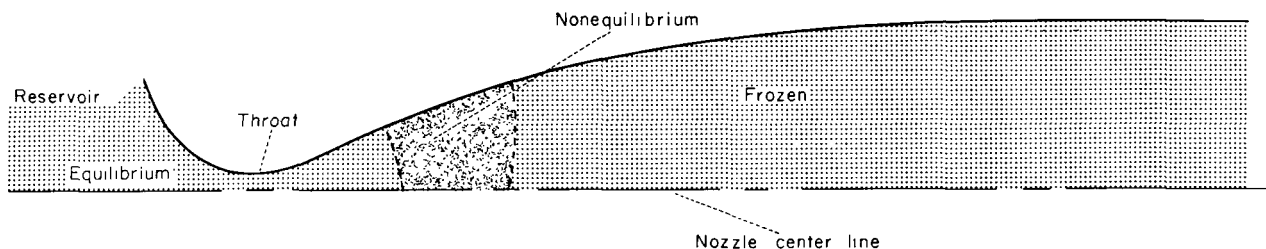


Figure IV-1.- Regions of flow in a typical high-speed nozzle.

In the region near the reservoir the high temperature of the air gives it a small relaxation time. In view of its small velocity, the air thus has an extremely short relaxation length here. In this region, therefore, the flow is in many cases in equilibrium. As the air approaches the throat the relaxation time greatly increases due to the dropping of the temperature. Also, the speed rapidly increases from subsonic toward supersonic values. Often, therefore, the relaxation length becomes moderate in the vicinity of the throat, and, if the relaxation length becomes moderate before the dissociated atoms have recombined, nonequilibrium conditions exist. As the air continues downstream, the relaxation length becomes large, and a near-frozen condition may exist at the exit of the nozzle.

#### Gas Model

In the preceding work to keep the discussion general, we have not been explicit as to the particular type of nonequilibrium, nor have we specified the actual equation of state. Now, to obtain a particular solution by numerical methods, we must decide on the gas model. A gas model that is a good approximation to real air for a moderate range of temperatures, and yet relatively simple, is a mixture of dissociating oxygen and nondissociating nitrogen. The molecular vibration is assumed to be at equilibrium, as are the molecular translation and rotation. The expressions for the thermodynamic and chemical-kinetic properties

of this simplified air are briefly derived in appendix A. In this derivation, the contribution of electronic excitations to the internal energy is neglected. This is equivalent to assuming the electronic partition functions to be constant, which is valid for the temperature range concerned ( $T < 8000^\circ \text{K}$ ).

The difference of the present air model from the Lighthill ideal dissociating gas (refs. 25 and 26) is due mainly to the inclusion of the dissociatively inert nitrogen. The principal approximation made in the Lighthill gas model, that  $\rho_D$  (defined by eq. (A-5)) is constant, is rather good for the range of temperature where dissociation is important. The Lighthill gas model, however, is not a good approximation for air for the present purpose because it has too high a value of  $a_f/a_e$ , which is an important parameter in estimating the nonequilibrium effects. The use of too high a value of  $a_f/a_e$  would lead to an overestimate of the effects of nonequilibrium.

The simplicity of the present air model, as compared with more complex ones, is due mainly to the fact that there is only one nonequilibrium process. For the higher temperature range where dissociation of nitrogen is important, an equally simple but not as good approximation for air would be a mixture of dissociating nitrogen and fully dissociated oxygen.

### Nozzle Model

The dimensions of the nozzle used in the present computations are shown in figure IV-2. The nozzle has a conical portion after the throat, followed by a fourth-degree-polynomial curved portion that matches the slope at the end of the conical section and has zero slope and curvature at  $x = 10.35 \text{ cm}$ . The conical section is included because a method of computation for the transonic throat

#### Notes

- 1 Curved portion at nozzle described by  
radius =  $0.21256x - 0.018783x^2 + 0.00014226x^3 + 0.000031201x^4$
- 2 Throat at  $x = 0.2352 \text{ cm}$ ; radius at throat =  $0.05 \text{ cm}$
- 3 Expansion area ratio at exit = 387.75

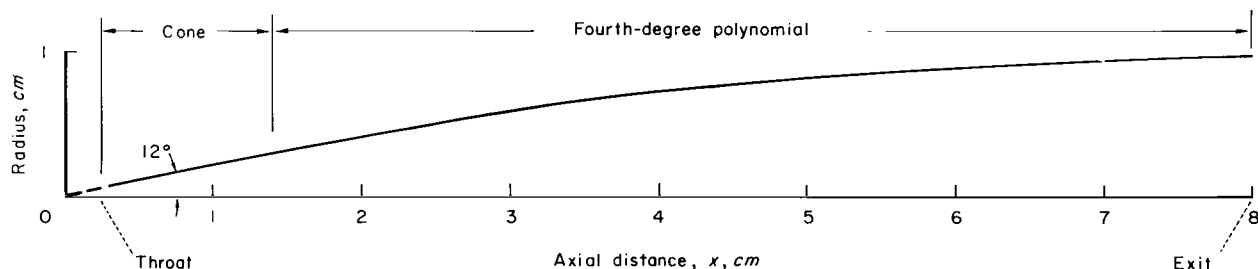


Figure IV-2.- Nozzle used in flow computations.

region is not available. If the conical section is large enough compared with the throat region, however, it is reasonable to assume that the flow itself is conical at the end of such a section. We select a fourth-degree-polynomial contour so that we can specify that the conical and the curved portions of the nozzle have matching slopes at their junction and that the curved portion has zero slope and curvature a short distance downstream from the nozzle exit. The selection of the location of the exit is described in the next paragraph. Such a nozzle may be thought of as representing the core of inviscid flow in a high-speed wind tunnel when the flow behavior differs (in the inviscid core or in the viscous layer, or both) from the design condition of uniform exit flow. In reality, the presence of a thick boundary layer in a wind-tunnel nozzle, such as the one we are considering, makes it difficult to achieve an exactly uniform flow in the test section under any condition, equilibrium or otherwise.

Since this nozzle is not ideally designed, that is, its wall is not so contoured that the exit flow is uniform for a particular initial condition, there is no assurance that the flow can turn uniformly to a parallel flow at the exit for any initial condition. Recompression (i.e., deceleration of the flow) may occur, as indeed it does for the present initial conditions used. This recompression is avoided by arbitrarily taking the nozzle exit to be a short distance upstream from where the nozzle wall becomes horizontal. We thus select the exit to be at  $x = 8$  cm.

The numerical method of computation is the well-known method of characteristics. The necessary basic relations for the computation (eqs. (III-1)) have already been developed in chapter III. In finite-difference form, these equations are (with reference to fig. IV-3)

$$\beta_{fAD}(p_D - p_A) + (\rho w^2)_{AD}(\theta_D - \theta_A) + \left( \frac{v}{M_{fr}} - 1 \right) \rho w^2 \sin \theta - \frac{h_\alpha}{M_{fr} h_p} w w \Big)_{AD} \Delta_{AD} = 0 \quad (IV-1a)$$

$$\beta_{fBD}(p_D - p_B) - (\rho w^2)_{BD}(\theta_D - \theta_B) + \left( \frac{v}{M_{fr}} - 1 \right) \rho w^2 \sin \theta - \frac{h_\alpha}{M_{fr} h_p} w w \Big)_{BD} \Delta_{BD} = 0 \quad (IV-1b)$$

$$(\rho w)_{CD}(w_D - w_C) + (p_D - p_C) = 0 \quad (IV-1c)$$

$$(\alpha_D - \alpha_C) - \left( \frac{\omega}{\bar{w}} \right)_{CD} \Delta_{CD} = 0 \quad (IV-1d)$$

where single-letter subscripts refer to locations and double-letter subscripts signify average values, except with  $\Delta$ , which is the linear distance between the two points referred to by the subscripts. Points A, B, and C are locations at which the values are known. Point D is the location at which the flow properties are to be found. Here  $\alpha$  is the degree of dissociation of oxygen.

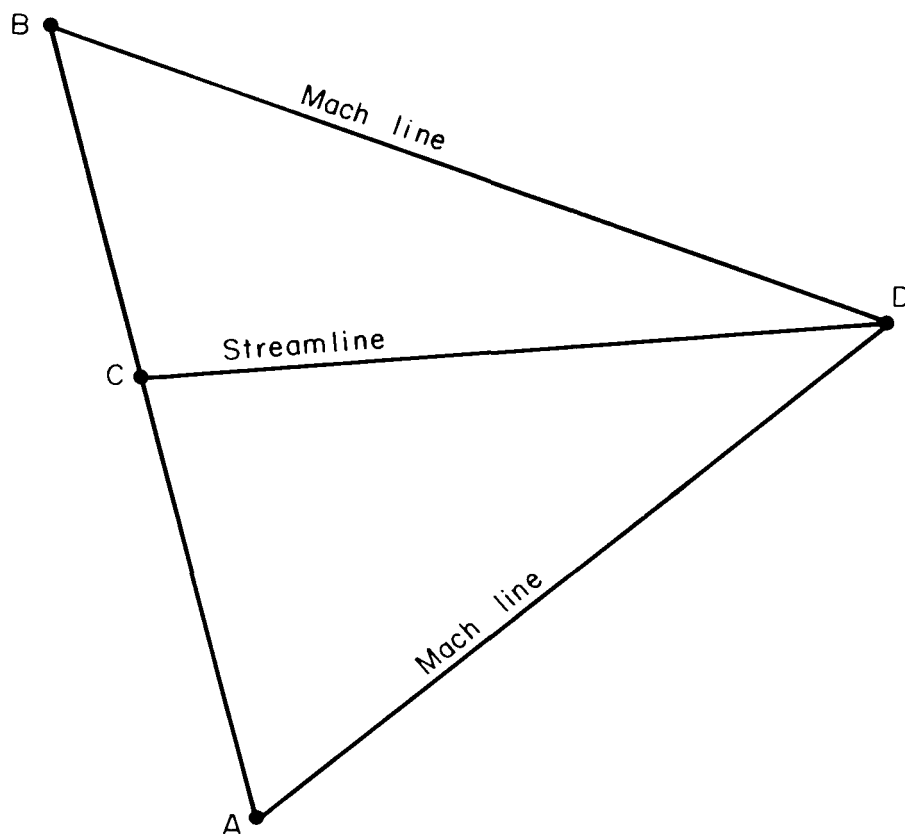


Figure IV-3.- Characteristics net for nonequilibrium-flow computations.

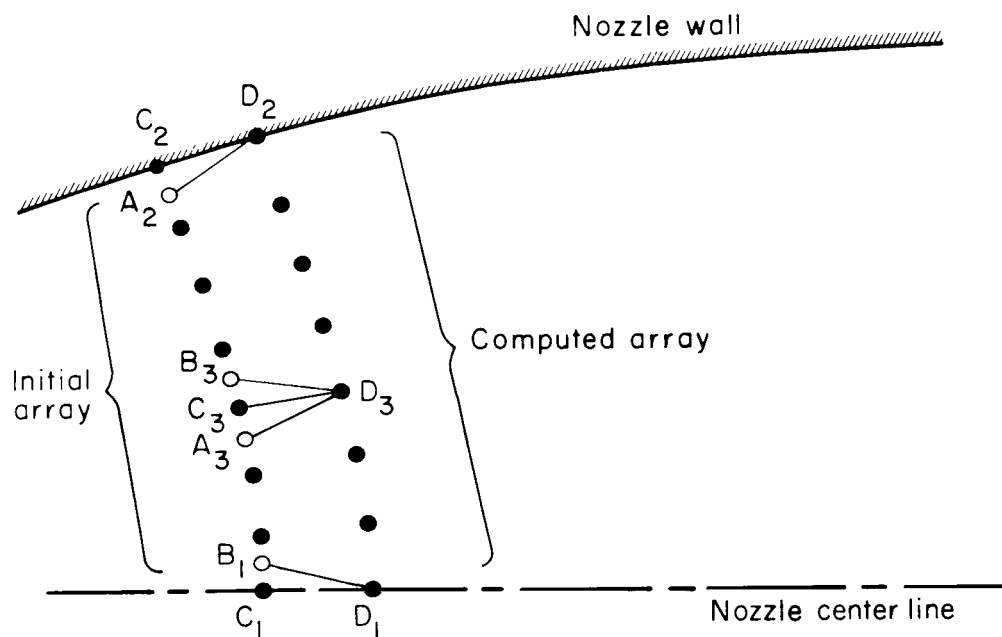


Figure IV-4.- Computation net for points on the nozzle center line, nozzle wall, and in the interior.

At the nozzle wall, equation (IV-1a) is replaced by  $\theta_D = \tan^{-1} \delta(x_D)$ , where  $\delta(x)$  is the slope of the nozzle wall. At the nozzle center line, equation (IV-1b) is replaced by  $\theta_D = 0$ .

The numerical procedure is as follows (cf. fig. IV-4): The values of  $p$ ,  $\theta$ ,  $w$ , and  $\alpha$  are taken to be known at each point, represented by the solid dots, in the initial array. We shall call those points the data points. Points  $D_1$ ,  $D_2$ , and points of type  $D_3$  constitute the array of points to be computed. For the nozzle center-line calculation,  $B_1$  is located halfway between data point  $C_1$  and the adjacent data point. The values of  $p$ ,  $\theta$ ,  $w$ , and  $\alpha$  at  $B_1$  are obtained by linear interpolation. Point  $D_1$  is located at the intersection of the nozzle center line and the right-running Mach line from  $B_1$ . For the nozzle wall calculation,  $A_2$  is located halfway between data point  $C_2$  and its adjacent data point, and  $D_2$  lies on the intersection of the nozzle wall and the left-running Mach line from  $A_2$ . The values of  $p$ ,  $\theta$ ,  $w$ , and  $\alpha$  at  $A_2$  are again obtained by linear interpolation. Finally, for a typical calculation that involves neither the nozzle wall nor center line,  $A_3$  is located halfway between data point  $C_3$  and the data point below it. Points of type  $D_3$  are then taken to lie on the intersection of the streamline from  $C_3$  and the left-running Mach line from  $A_3$ , and  $B_3$  at the intersection of the right-running Mach line through  $D_3$  and the straight line connecting  $C_3$  with the data point next above it. The values of  $p$ ,  $\theta$ ,  $w$ ,  $\alpha$  at  $A_3$  and  $B_3$  are obtained by linear interpolation.

For the starting of the integration process, the values of  $p$ ,  $\theta$ ,  $w$ ,  $\alpha$  for points  $D_1$ ,  $D_2$ , and type  $D_3$  are the same as those for points  $C_1$ ,  $D_2$ , and type  $C_3$ , respectively. The numerical integration for points of type  $D_3$  involves solving equations (IV-1a) and (IV-1b) for  $p_{D_3}$  and  $\theta_{D_3}$ , then equations (IV-1c) and (IV-1d) for  $w_{D_3}$  and  $\alpha_{D_3}$ . The new values for  $p_{D_3}$ ,  $\theta_{D_3}$ ,  $w_{D_3}$ , and  $\alpha_{D_3}$  are used in recomputing the coefficients in the compatibility relations and in refining the locations of the points  $D_3$  and  $B_3$ . The values of  $p$ ,  $w$ ,  $\theta$ ,  $\alpha$  for  $B_3$  are then reinterpolated, and the values for  $p$ ,  $w$ ,  $\theta$ ,  $\alpha$  at  $D_3$  are recomputed. The computation process is then repeated. The iteration is continued until the velocity reaches a preassigned accuracy. For errors of  $10^{-4}$  percent (between successive iterations) or less in the velocity, it usually takes four iterations to compute one point. The computations for  $D_1$  and  $D_2$  are essentially the same except that one less computation is needed because the value of  $\theta$  is known at  $D_1$  and  $D_2$ . After the entire new array consisting of points  $D_1$ ,  $D_2$ , and type  $D_3$  are computed, the computed array is used as a new initial array.

There is very little improvement in the accuracy of the computed results once the number of points in an array exceeds 18. The grid sizes, which are dependent on the number of data points in each array, are selected to be as small as necessary to give the desired accuracy for the flow quantities at the nozzle exit. The selected number of data points in each array in the actual computation is roughly 30. The streamwise mesh size for a 30-point array is approximately 0.03 cm at the start of the nonequilibrium calculation. This mesh size is about one-half of the corresponding characteristic reaction length  $\tau_r w$ . The streamwise mesh size becomes larger as the flow proceeds downstream as a result of the

widening of the nozzle and the increasing of the Mach number. The streamwise mesh size at the exit is approximately 0.1 cm. The mesh size for all four cases computed (equilibrium and nonequilibrium) is about the same.

For frozen flow, equations (IV-1) are immediately applicable; the terms involving  $\omega$  in equations (IV-1a,b, and d) are simply zero. In the equilibrium limit, the term containing  $\omega$  in equation (II-4a) combines with the leading term to yield a quantity  $M_e^2 \partial p / \partial s$ . For the equilibrium flow, the compatibility equations become simply

$$\beta_{eAD}(p_D - p_A) + (\rho w^2)_{AD}(\theta_D - \theta_A) + \left( \frac{v - 1}{M_{er}} \rho w^2 \sin \theta \right)_{AD} \Delta_{AD} = 0 \quad (IV-2a)$$

$$\beta_{eBD}(p_D - p_B) - (\rho w^2)_{BD}(\theta_D - \theta_B) + \left( \frac{v - 1}{M_{er}} \rho w^2 \sin \theta \right)_{BD} \Delta_{BD} = 0 \quad (IV-2b)$$

and are essentially the same as those for frozen flow except that the Mach number and the corresponding characteristic directions are based on the equilibrium speed of sound.

The numerical computation described above was performed on the IBM 7090 computer of the Ames Research Center, NASA. The machine program is coded in FORTRAN language. Fourteen subroutines are used to facilitate both the machine program verification and any future modification such as using different gas models (as long as only one nonequilibrium process is allowed).

The numerical examples computed for the present study are based on a reservoir condition of  $T = 9000^\circ \text{K}$  and  $p = 1000$  atmospheres. Four cases were studied: equilibrium flow and three cases of nonequilibrium flow with the effective characteristic reaction time  $\tau_{\text{reft}}$  taken as 0.1, 1, and 10 times the value of  $\tau_r$  given by equation (A-9). The case of equilibrium flow has, of course, an effective characteristic reaction time of zero.

To obtain the initial conditions, we assume that the gas is in equilibrium up to the location at which the Mach number  $M_f$  is 1.1 and that ahead of this location the gas behaves like real air. This last assumption gives a starting condition (i.e., values of  $p$ ,  $\rho$ , and  $M_f$ ) corresponding exactly to real air with the reservoir conditions stated above. For the present computation these starting values of  $p$  and  $\rho$  are obtained from the charts prepared by Yoshikawa (ref. 27), and the corresponding value of  $\alpha = \alpha_e$  is computed using equation (A-4). The initial conditions are thus more realistic than those that would have been obtained using the simplified air model throughout, since at temperatures higher than those at the throat the nitrogen is dissociated. The assumption that the flow upstream of the location of  $M_f = 1.1$  is in equilibrium

is justified, since the subsequent computations show that the flow has no tendency to deviate from the equilibrium curve (fig. IV-5) until downstream of this point.

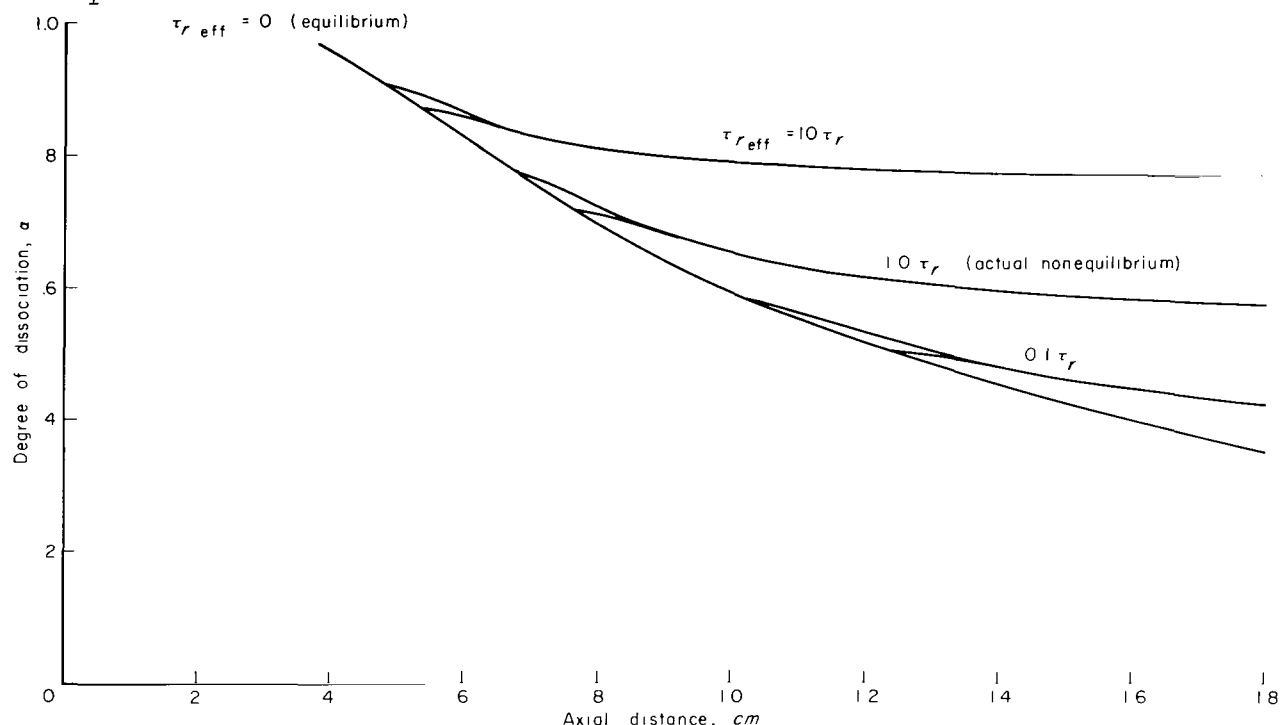


Figure IV-5.- Degree of dissociation along the nozzle center line in the transition region for various degrees of nonequilibrium and various assumed nonequilibrium starting positions.

The flow for the equilibrium condition is first computed. For a nonequilibrium calculation, the value of the effective characteristic reaction length  $\tau_{\text{reff}}^w$  from the equilibrium flow along the nozzle is then observed. Once  $\tau_{\text{reff}}^w$  becomes moderately long (in the present computations about twice the streamwise mesh size), the flow is assumed to be in a nonequilibrium condition, and the computation for nonequilibrium is used for the flow downstream of this point. To assure that the selected effective starting point for the nonequilibrium calculation is a correct one, at least one more case using a starting point upstream or downstream of it must be computed. The degree of dissociation along the nozzle center line in the transition region is presented in figure IV-5. As seen from this figure, for each effective  $\tau_r$ , there is a certain location ahead of which the nonequilibrium effect is so small that any point upstream of it can be used as an effective starting point without serious error in the transition region. The starting point cannot be too far upstream, however, since too high a reaction rate would make the numerical computation unstable.

The characteristic reaction length  $\tau_r^w$  for the equilibrium flow and the actual nonequilibrium flow (effective  $\tau_r = 1.0\tau_r$ ) is presented in figure IV-6. As seen from this, the characteristic length  $\tau_r^w$  increases rapidly in the

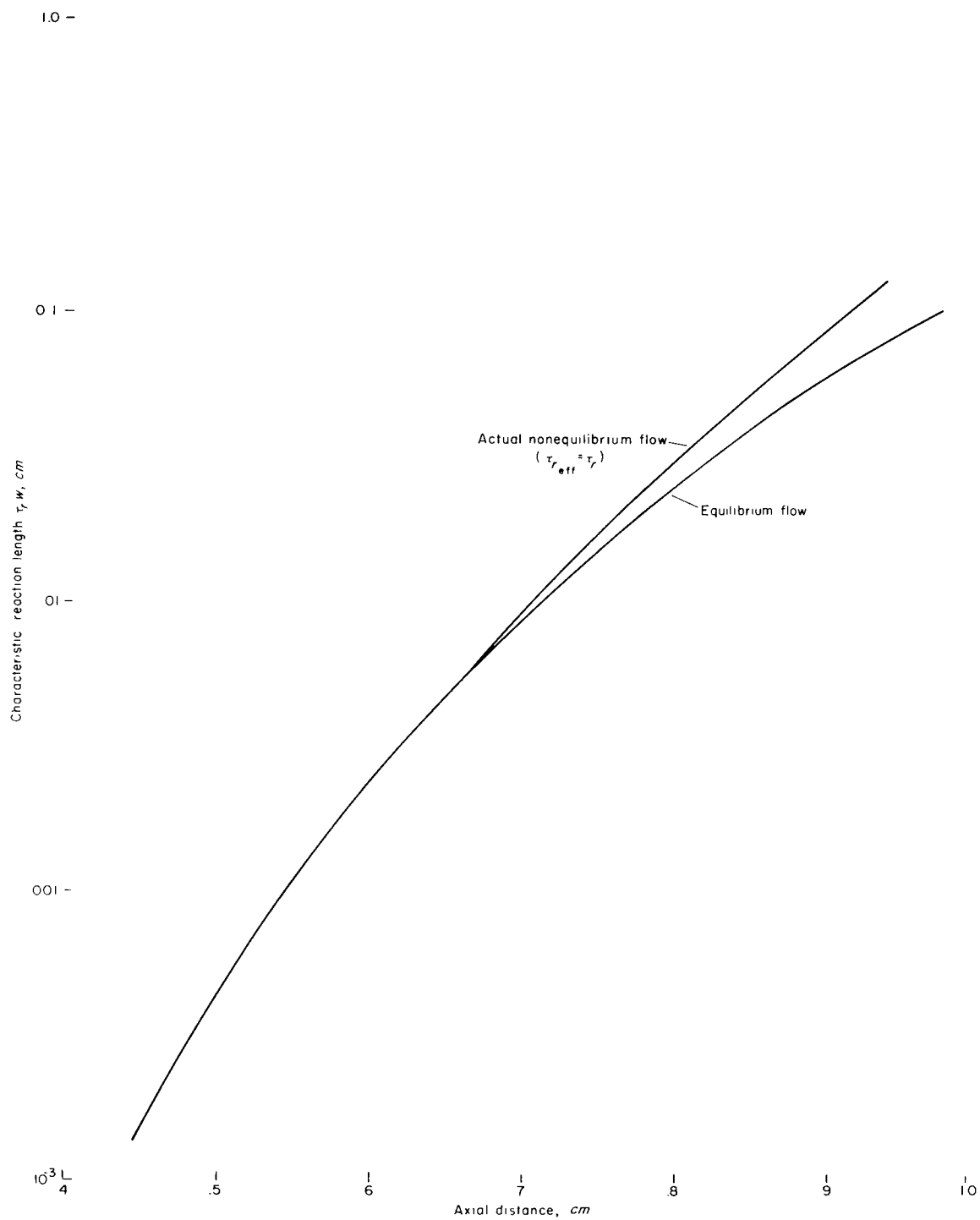


Figure IV-6.- Characteristic reaction length in the transition region of the nozzle.



region immediately after the throat, causing the flow to deviate from equilibrium. Later  $\tau_{rw}$  increases to values even larger than the physical length of the nozzle, and the flow becomes nearly frozen shortly past the conical section.

The variation of the flow quantities along the center line are presented in figures IV-7 through IV-11. These variations are qualitatively the same as those from calculations of quasi-one-dimensional flow (refs. 5, 8, and 9). Thus, quasi-one-dimensional-flow computations can give an assessment of the effects of nonequilibrium, at least qualitatively.

Note that while all flow quantities along the center line deviate from the equilibrium-flow values, the extent of the deviation depending on the effective reaction rate, the deviation of the velocity (fig. IV-8) is relatively slight. This phenomenon may be useful for some approximations. The temperature (fig. IV-10), on the other hand, deviates considerably from the equilibrium-flow value, causing the Mach number (fig. IV-11) to deviate correspondingly.

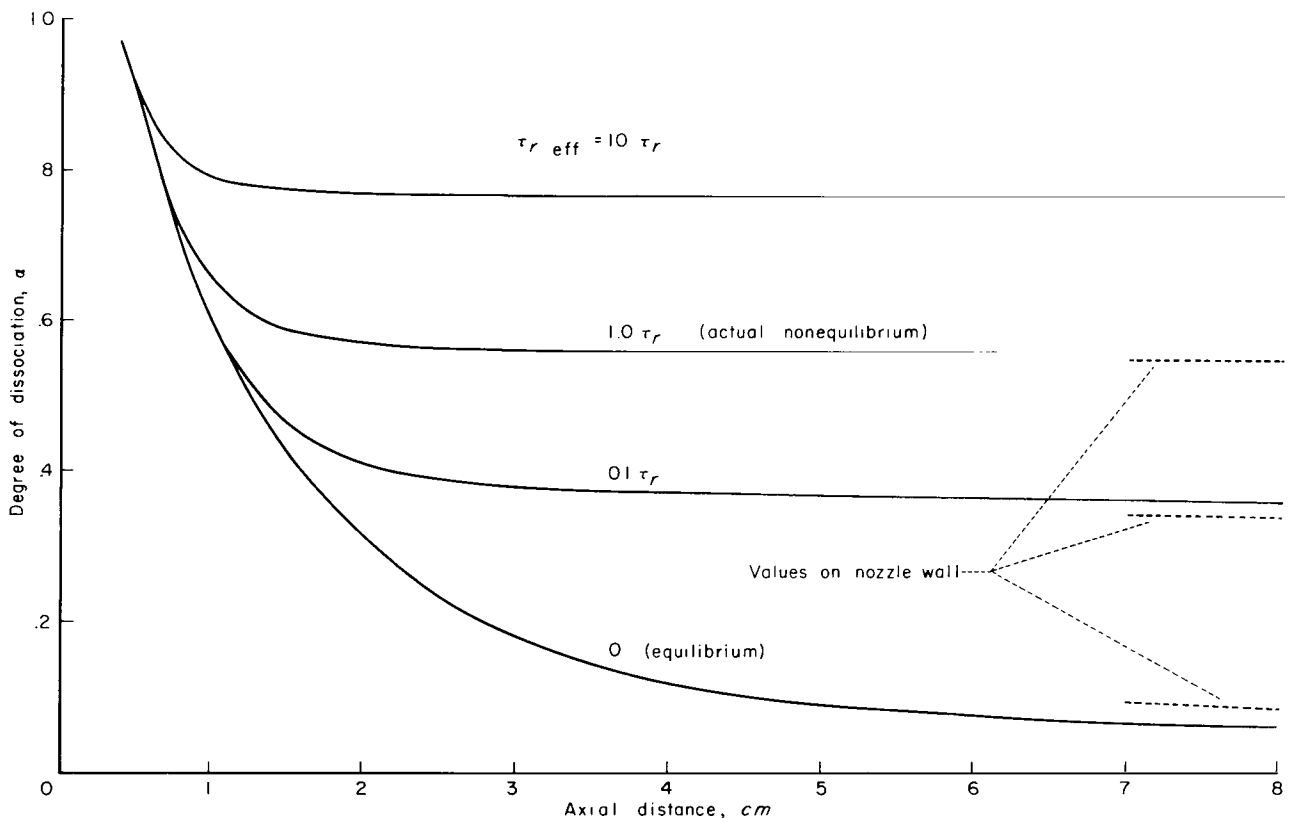


Figure IV-7.- Degree of dissociation along the nozzle center line for various degrees of nonequilibrium.

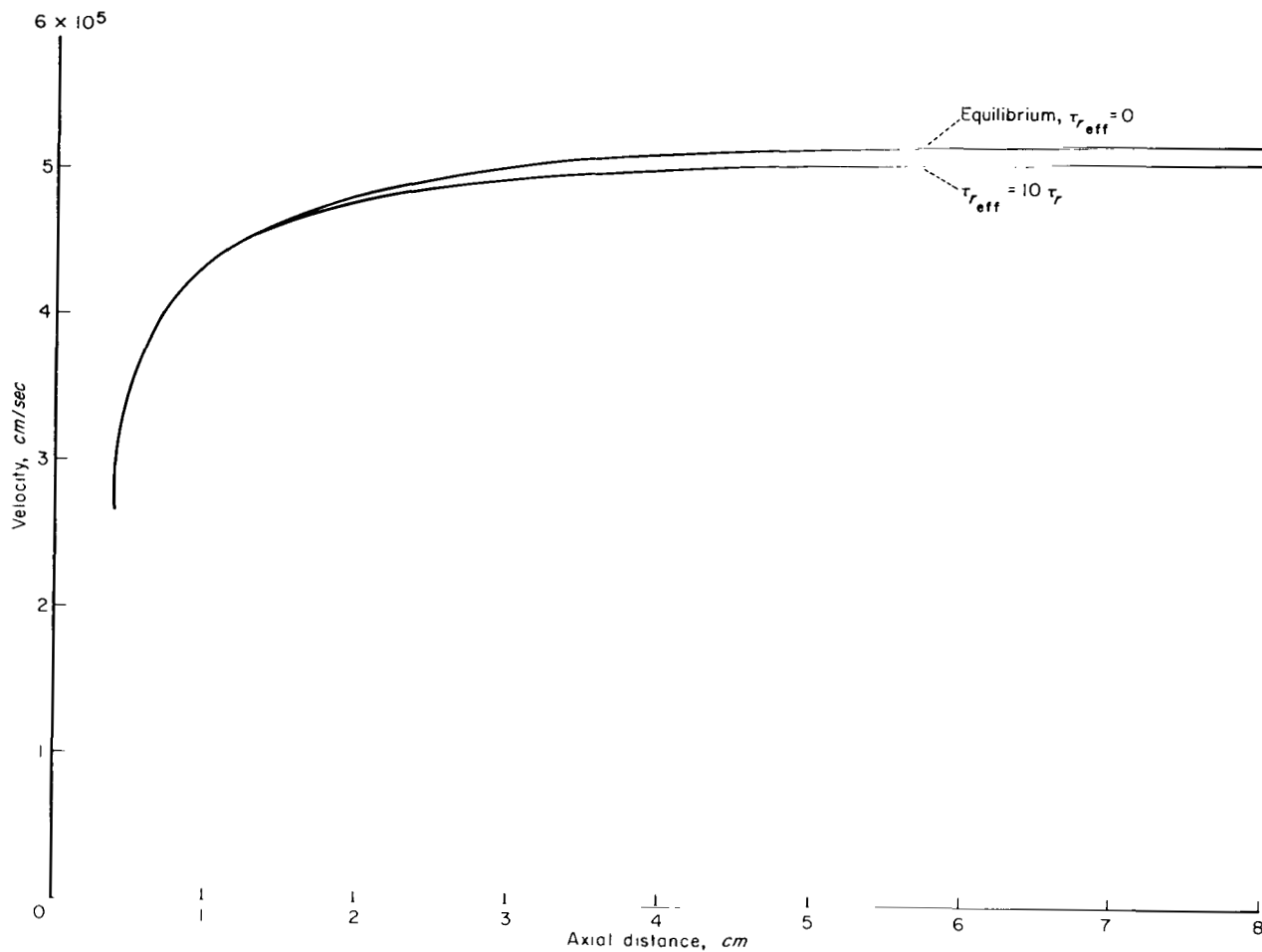


Figure IV-8.- Velocity along the nozzle center line for equilibrium and nonequilibrium flow.

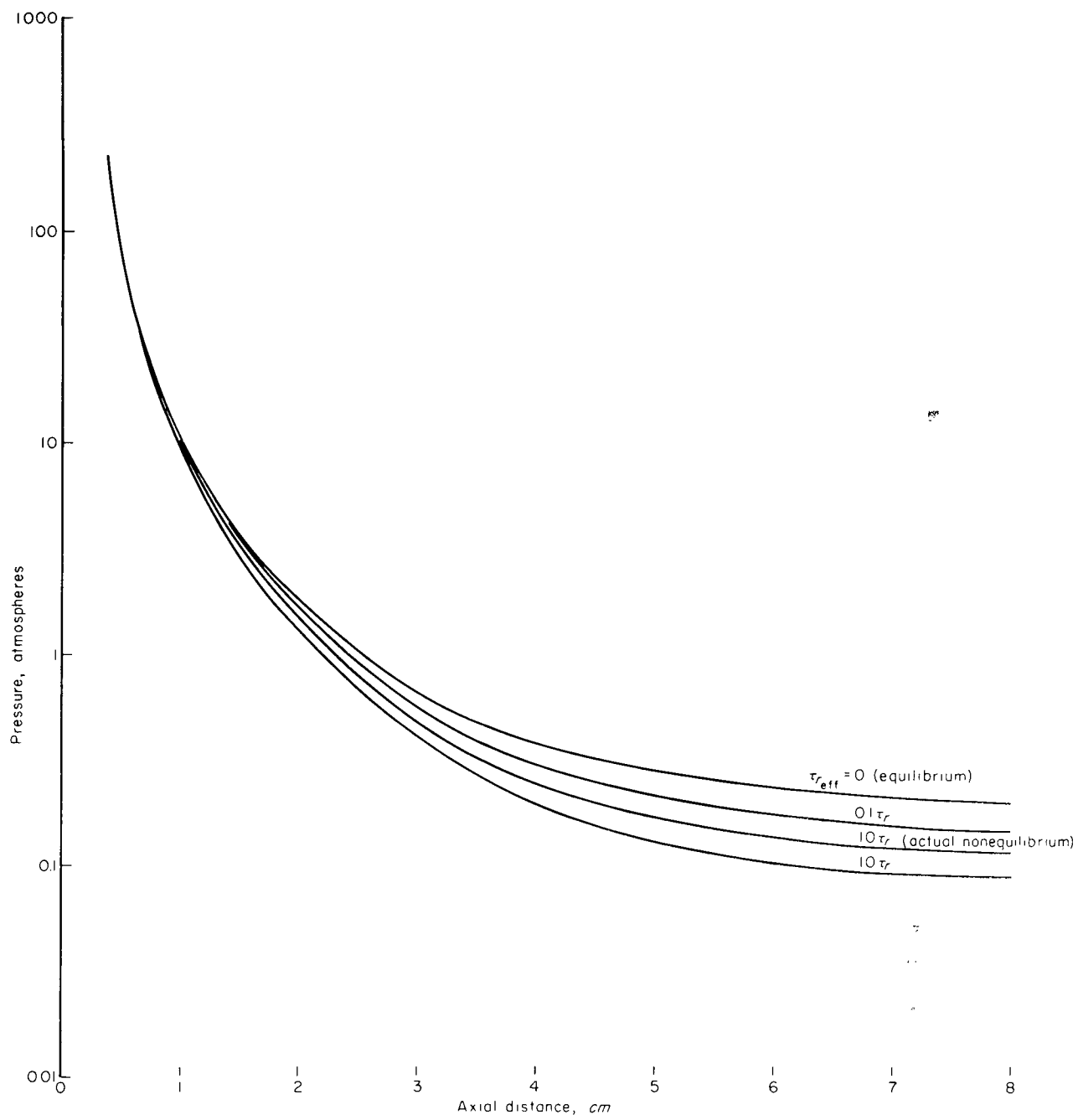


Figure IV-9.- Pressure along the nozzle center line at various degrees of nonequilibrium.

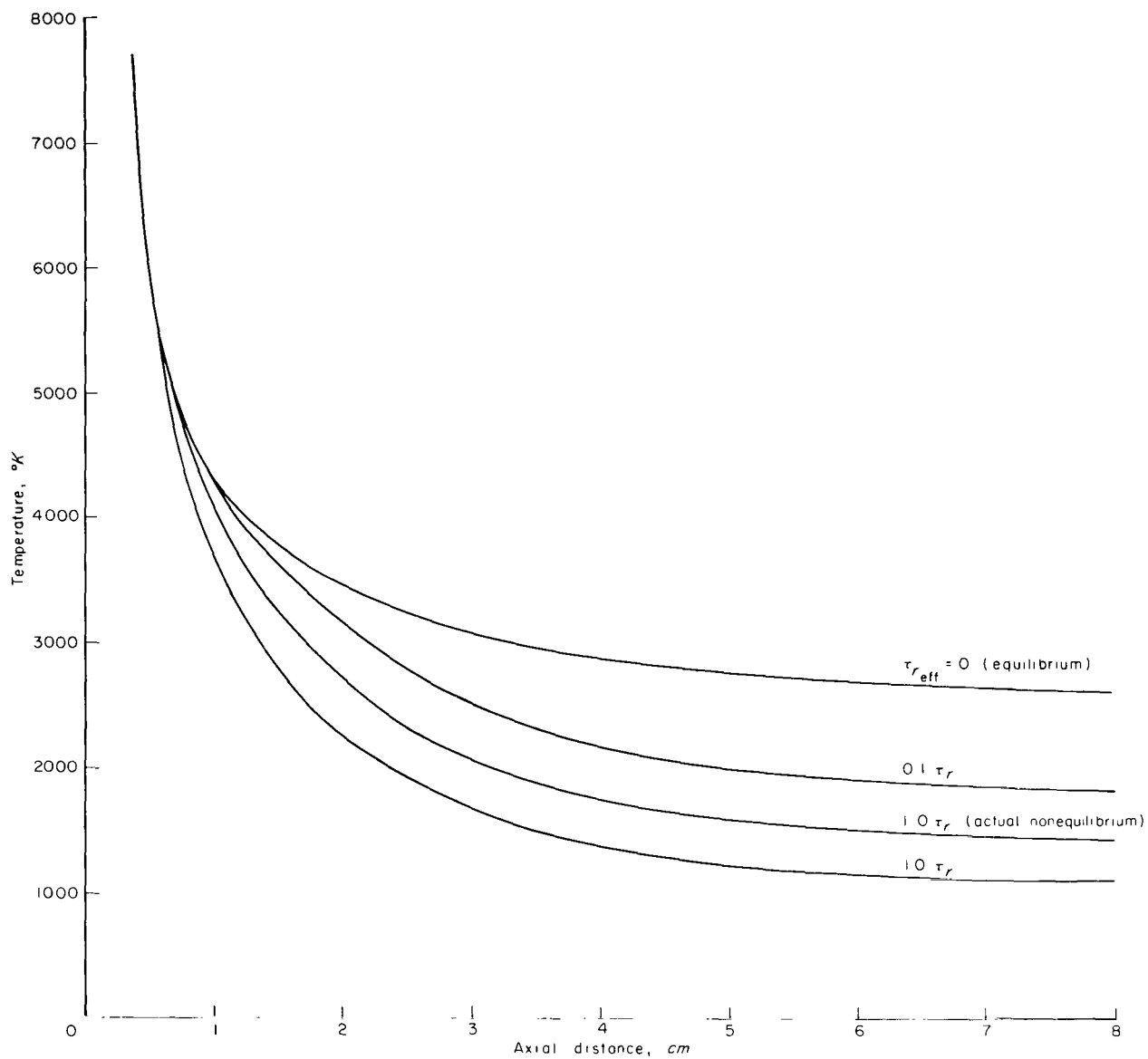


Figure IV-10.- Temperature along the nozzle center line for various degrees of nonequilibrium.

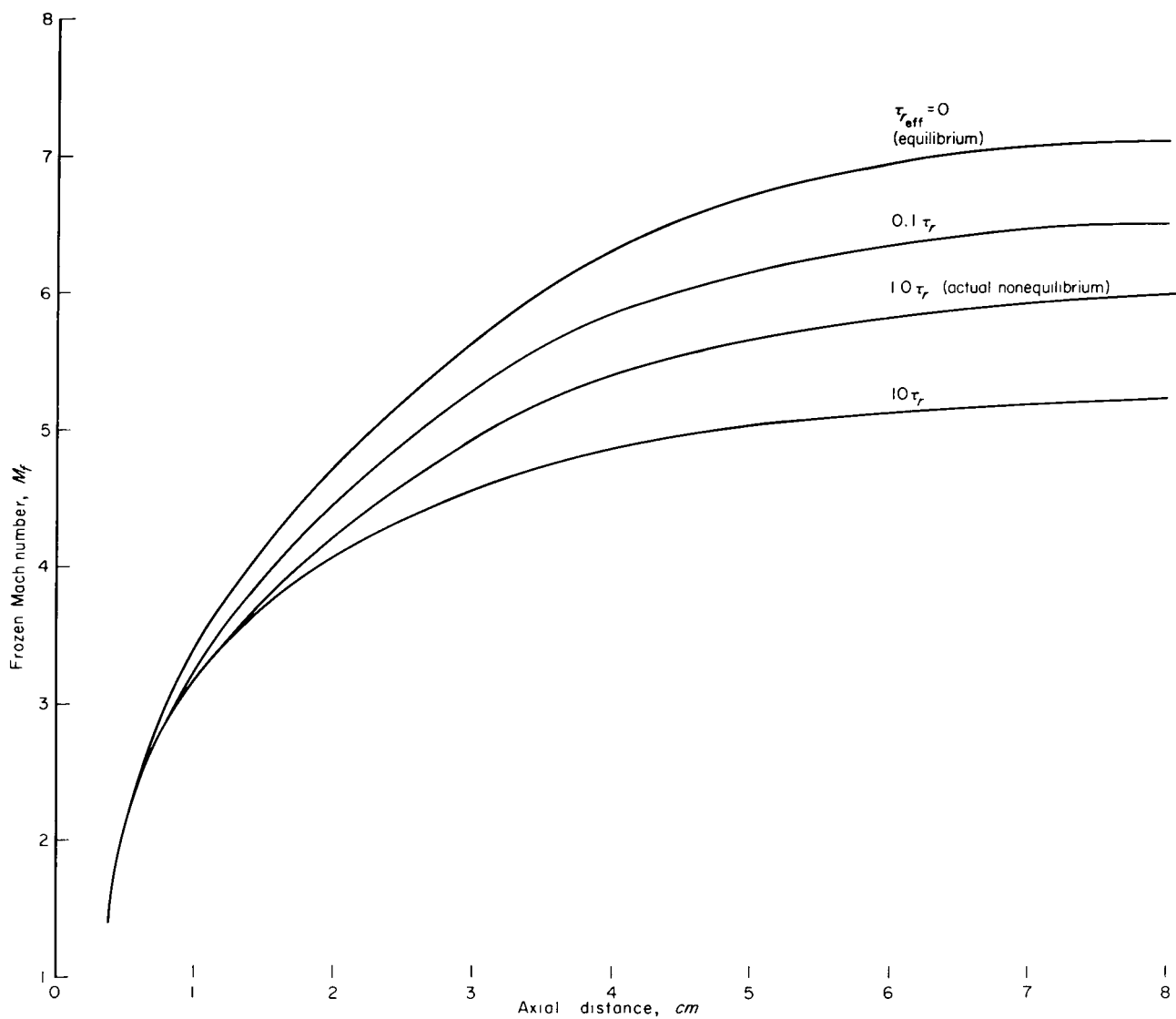


Figure IV-11.- Frozen Mach number along the nozzle center line for various degrees of nonequilibrium.

The gas next to the nozzle wall travels a longer distance than that on the nozzle center line. Furthermore the flow on the center line expands more rapidly and hence freezes sooner. It may be conjectured, therefore, that the flow remains closer to equilibrium at the wall than at the center. If the flow is significantly out of equilibrium, then, the value of  $\alpha$  at the wall should be lower than that at the center. If the flow is near equilibrium, of course, the value of  $\alpha$  is lower at the nozzle center line than that at the wall simply because the flow along the center line expands more. This is shown to be the case in figure IV-7.

The variations of the flow properties across the nozzle-exit plane are presented in figures IV-12 through IV-16. These figures show that, in general (except  $\alpha$ ), the nonuniformities become more pronounced as the effective value of  $\tau_r$  increases, that is, as the flow tends toward the frozen condition.

The velocity, fairly uniform when the flow is in equilibrium (fig. IV-13), stays fairly uniform when the flow is out of equilibrium. Note that, although  $\alpha$  varies across the exit plane (fig. IV-12), the corresponding values of  $Z = 1 + (\alpha/4.764)$ , which dictates the relative importance of dissociation in the thermal equation of state, are actually fairly constant. Pressure (fig. IV-14), on the other hand, has a deviation from the center to the nozzle wall some 30 percent (when effective  $\tau_r = 1.0\tau_r$ ) more than the equilibrium case.

We may therefore conjecture that, since we cannot in the design of a nozzle by the inverse method have all of the exit quantities exactly uniform when the flow is out of equilibrium, we will attain the over-all best uniformity by taking the pressure uniform, the streamlines parallel ( $\theta = 0$ ), and the velocity and  $\alpha$  unspecified. We may conjecture, also, that for a nozzle designed to give a uniform flow at the exit for equilibrium conditions, the pressure and Mach number may vary significantly from the nozzle center to the wall if the flow turns out to be nonequilibrium.

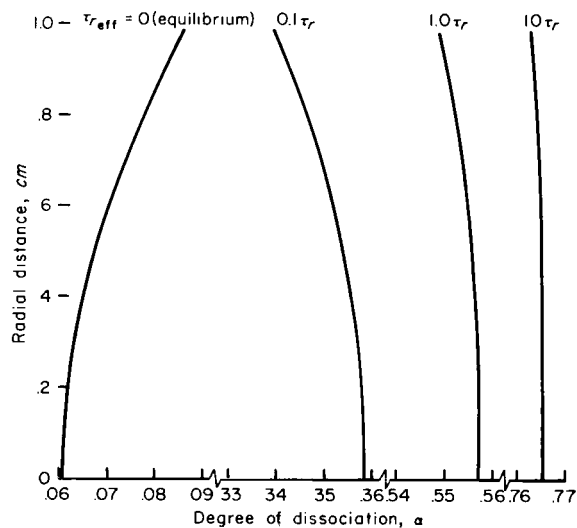


Figure IV-12.- Variation of degree of dissociation across the nozzle-exit plane.

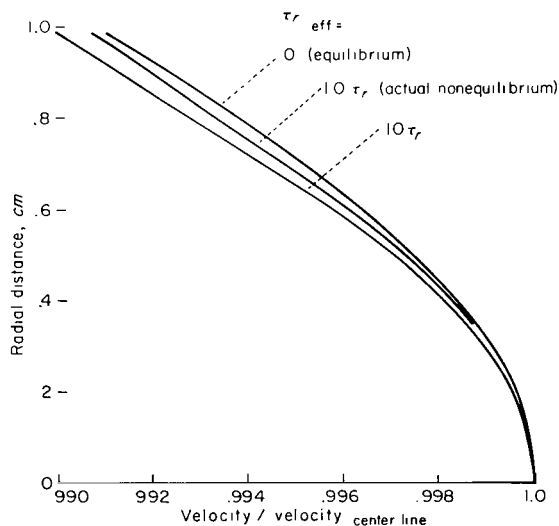


Figure IV-13.- Velocity distribution across the nozzle-exit plane.

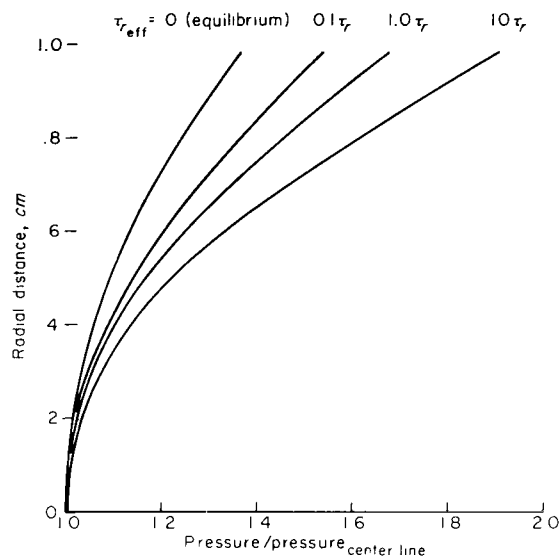


Figure IV-14.- Pressure distribution across the nozzle-exit plane.

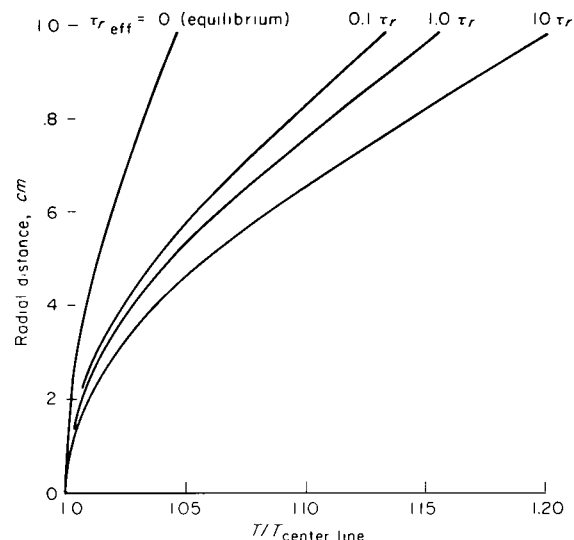


Figure IV-15.- Temperature distribution across the nozzle-exit plane.

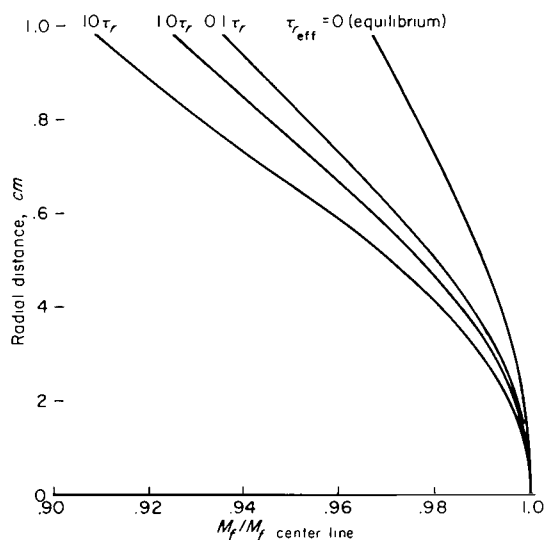


Figure IV-16.- Frozen Mach number distribution across the nozzle-exit plane.

flow is not quasi-one-dimensional is essentially frozen), complete uniformity at the nozzle exit can be prescribed. This would provide one method of designing an ideal nozzle for nonequilibrium flow.

Lastly, the useful, approximate, sudden-freeze analysis for nonequilibrium flow (ref. 6), which was developed for quasi-one-dimensional flow, can be adopted for axisymmetric flow. This can be done by switching from a computation

In the present case, the correct nonequilibrium flow ( $\tau_{\text{eff}} = \tau_r$ ) is nearly frozen shortly after it passes the conical section, which here is a relatively small portion of the nozzle. If a longer conical section were prescribed, the flow would be nearly frozen at the end of the cone. Then one would compute the conical part by quasi-one-dimensional flow, which is exact in this region, and determine the flow in the rest of the nozzle by a frozen, axisymmetric computation for a thermally perfect gas (for which  $\alpha$  and hence  $z$  are constants). Such calculations are readily made since the methods for both the nonequilibrium quasi-one-dimensional flow and the thermally perfect axisymmetric flow have already been developed. Furthermore, if the conical section is large enough that effective freezing starts before the end of the conical section (so that the region in which the

of equilibrium flow to one of frozen flow when appropriate conditions are reached on each streamline. If freezing occurs after the flow passes the conical portion of the nozzle, the center line will freeze first because of more rapid expansion there. Since along each cross section the flow at the center tends to freeze first, the computation along curve AD (in fig. IV-3) will reach the condition for sudden freezing sooner than that along CD. This should cause no difficulty, for one can use an equilibrium-flow computation along BD and CD together with a frozen-flow computation along AD without incompatibility.

Ames Research Center

National Aeronautics and Space Administration

Moffett Field, Calif., Nov. 15, 1962



## APPENDIX A

### THERMODYNAMIC AND CHEMICAL-KINETIC PROPERTIES OF A SIMPLIFIED

#### AIR MODEL

In this section we set down the thermal and caloric equations of state, the rate equation, and the expressions for the auxiliary properties, such as the speeds of sound, that appear in the coefficients of the flow equations. We will consider only the simplified air model described briefly in chapter IV. In this gas model the air is assumed to be a mixture of oxygen and nitrogen with only the oxygen dissociated. The translation, rotation, and vibration of each constituent are taken to be in equilibrium (i.e., they have a Maxwell-Boltzmann distribution), and the electronic excitation is assumed negligible. The derivation of the properties of this gas is straightforward. Only minimum details, enough to indicate the assumptions involved, will be given since derivations for more complicated gas models are available (e.g., refs. 22, 28, and 29).

The number density (number of particles per unit mass of gas mixture) for the constituents in the mixture are

$$n_O = \frac{\alpha}{m_O(1 + a)}$$

$$n_{O_2} = \frac{1 - \alpha}{2m_O(1 + a)}$$

$$n_{N_2} = \frac{a/b}{2m_O(1 + a)}$$

where  $\alpha$  is the ratio of the mass of oxygen in atomic form to the total mass of atomic and molecular oxygen,  $a$  is the ratio of the mass of nitrogen to the mass of the oxygen in the mixture,  $b$  is the ratio of the atomic weight of nitrogen to that of oxygen, and  $m_O$  is the mass of an oxygen atom. The actual values used for the constants are listed in table I at the end of appendix A.

The assumption that the translation of the molecules has a Maxwell-Boltzmann distribution permits us to write the thermal equation of state as

$$\frac{p}{\rho} = kT(n_O + n_{O_2} + n_{N_2})$$

where  $k$  is the Boltzmann constant. Substituting the relation for  $n_0$ ,  $n_{O_2}$ ,  $n_{N_2}$ , and letting  $R \equiv [1 + (a/b)]k/[2m_0(1 + a)]$ , and  $Z \equiv 1 + \alpha[1 + (a/b)]^{-1}$ , we have

$$\frac{p}{\rho} = ZRT \quad (A1)$$

The specific internal energy  $e$ , with the zero energy of the mixture taken to be that of the atomic species at absolute zero temperature, is the sum of the translational, rotational, and vibrational energies of the species (since electronic excitation is neglected). We thus write

$$e = \sum_i n_i (E_{\text{translation}_i} + E_{\text{rotation}_i} + E_{\text{vibration}_i} - E_{\text{dissociation}_i})$$

where the subscript  $i$  takes the values 1, 2, 3 corresponding to the species O,  $O_2$ ,  $N_2$ , respectively. Substituting the values of  $n_i$  and denoting  $E_{\text{dissociation}_i}/k$  by  $\Theta_{D_i}$ , we have, for the enthalpy  $h = e + p/\rho$ , with  $E_{\text{translation}_i} = (3/2)kT$  and (assuming rotation fully excited)  $E_{\text{rotation}_i} = kT$

$$h = \left(1 + \frac{a}{b}\right) \left(2 + \frac{3}{2} Z\right) RT + R \left\{ \frac{1}{k} \left[ (1 - \alpha) E_{\text{vib}_{O_2}} + \left(\frac{a}{b}\right) E_{\text{vib}_{N_2}} \right] + \left[ (1 - \alpha) \Theta_{D_{O_2}} + \frac{a}{b} \Theta_{D_{N_2}} \right] \right\} \quad (A2)$$

where  $E_{\text{vib}_i}$  is given by the relation

$$E_{\text{vib}_i} = \frac{k\Theta_{V_i} \exp(-\Theta_{V_i}/T)}{1 - \exp(-\Theta_{V_i}/T)}$$

Here  $\Theta_{V_i}$  is the characteristic vibrational temperature.

The rate of change of the degree of dissociation  $\alpha$  can be obtained by summing the forward and reverse reaction rates of oxygen in the presence of atomic oxygen and molecular oxygen and nitrogen. Here the rate equation differs from equation (7.34) of reference 22 only by the additional term due to the presence of nitrogen as a catalytic species. The rate equation thus takes the form

$$\frac{d\alpha}{dt} = \frac{\rho}{M_0(1 + a)} \left[ \alpha k_{fO} + \frac{1 - \alpha}{2} k_{fO_2} + \frac{1}{2} \frac{a}{b} k_{fN_2} \right] \left[ 1 - \alpha - \frac{2\rho\alpha^2}{M_0 K_c(1 + a)} \right] \quad (A3)$$

where  $M_0$  is the atomic weight of oxygen, the subscripts for  $k_{fi}$  denote the particular catalytic species, and  $K_c$  is the equilibrium constant. The quantity inside the last bracket is, from the law of mass action, zero when  $\alpha$  has its equilibrium value  $\alpha_e$ . Thus we have

$$\frac{\alpha_e^2}{1 - \alpha_e} = \frac{\rho_D(T)}{\rho} \exp\left(-\frac{\Theta_{D_{O_2}}}{T}\right) \quad (A4)$$

where

$$\rho_D(T) = \frac{(1 + a)M_0}{2} K_c \exp\left(\frac{\Theta_{D_{O_2}}}{T}\right) \quad (A5)$$

The value of  $K_c$  can be expressed by means of the partition function. In terms of temperature, we have

$$K_c = \frac{2m_0}{M_0} \left(\frac{\pi m_0 k}{h^2}\right)^{3/2} \Theta_{r_{O_2}} \sqrt{T} \left(1 - \exp\left(-\frac{\Theta_{v_{O_2}}}{T}\right)\right) \frac{(p.f.)_{O_{el}}^2}{(p.f.)_{O_{2el}}} \exp\left(-\frac{\Theta_{D_{O_2}}}{T}\right) \quad (A6)$$

where  $h$  is the Planck constant and  $\Theta_{r_{O_2}}$  is the characteristic rotational temperature for oxygen. The ratio of the electronic partition functions is assumed to be constant, consistent with the earlier assumption of neglecting the contribution of electronic excitation to the internal energy. The value of this ratio is taken to be 24.42.

We use the same rate constants adopted by Hall (ref. 10). They are

$$k_{f_{O_2}} = 3.56 \times 10^{21} T^{-3/2} \exp\left(-\frac{\Theta_{D_{O_2}}}{T}\right), \text{ cm}^3/\text{mole sec} \quad (A7a)$$

$$\frac{k_{f_O}}{k_{f_{O_2}}} = \frac{35T}{\Theta_{D_{O_2}}} \quad (A7b)$$

$$\frac{k_{f_{N_2}}}{k_{f_{O_2}}} = \frac{1}{3} \quad (A7c)$$

where  $\Theta_{D_0}$  has the value  $59,380^\circ \text{ K}$ . The total forward reaction rate constant, that is, the quantity inside the first bracket of equation (A3), is thus

$$k_f = \left(\frac{35\alpha T}{\Theta_{D_{O_2}}} + \frac{1 - \alpha}{2} + \frac{1}{6} \frac{a}{b}\right) k_{f_{O_2}} \quad (A8)$$

The reciprocal of the entire quantity multiplying the last bracket of equation (A3) has the dimensions of time and characterizes the time it takes for the chemical reaction to reach equilibrium. This quantity, the characteristic reaction time, will be denoted as  $\tau_r$ , that is

$$\tau_r = (1 + a)M_0/\rho k_f \quad (A9)$$

There remain now only the frozen speed of sound  $a_f$  and the equilibrium of speed of sound  $a_e$ . These are given by the identities (ref. 22)

$$a_f^2 \equiv \frac{h_\rho}{\rho^{-1} - h_p} \quad (A10)$$

$$a_e^2 \equiv \frac{h_\rho + h_\alpha \alpha_{e\rho}}{\rho^{-1} - (h_p + h_\alpha \alpha_{e\rho})} \quad (A11)$$

where the subscripts  $p, \rho, \alpha$  denote partial differentiations, for example,  $h_p \equiv (\partial h / \partial p)_{\rho, \alpha}$ ,  $\alpha_{e\rho} \equiv (\partial \alpha_e / \partial \rho)_p$ . Thus they are simply related to the derivatives of  $h$  and  $\alpha_e$ . If we denote the quantity in the right-hand side of equation (A2) by  $f(\alpha, T)$ , then  $h_p$  is simply

$$h_p \equiv \left( \frac{\partial h}{\partial p} \right)_{\rho, \alpha} = \left( \frac{\partial f}{\partial T} \right)_\alpha \left( \frac{\partial T}{\partial p} \right)_{\rho, \alpha} = \frac{T}{p} \left( \frac{\partial f}{\partial T} \right)_\alpha$$

whereas  $h_\rho$  and  $h_\alpha$  are

$$h_\rho = - \frac{T}{\rho} \left( \frac{\partial f}{\partial T} \right)_\alpha$$

$$h_\alpha = -T \left[ \left( 1 + \frac{a}{b} \right) Z \right]^{-1} \left( \frac{\partial f}{\partial T} \right)_\alpha + \left( \frac{\partial f}{\partial \alpha} \right)_T$$

In a similar manner, if we denote  $\log[\rho_d(T) \exp(-\Theta_{D_{O_2}}/T)]$  by  $f_2(T)$ , then  $\alpha_{e\rho} \equiv (\partial \alpha_e / \partial \rho)_p$  and  $\alpha_{ep} \equiv (\partial \alpha_e / \partial p)_\rho$  can be obtained by differentiating equation (A4) (with the aid of eq. (A1)) as

$$\begin{aligned} \alpha_{e\rho} &= \frac{f_2(\partial T / \partial \rho)_{p, \alpha} - (1/\rho)}{[(2 - \alpha_e)/\alpha_e(1 - \alpha_e)] - f_2(\partial T / \partial \alpha)_{p, \rho}} \\ &= -(1 + f_2 T) \left( \rho \left\{ \frac{2 - \alpha_e}{\alpha_e(1 - \alpha_e)} - \frac{f_2}{[1 + (a/b)] + \alpha_e} \right\} \right)^{-1} \end{aligned}$$

and

$$\alpha_{ep} = f_2 T \left( p \left\{ \frac{2 - \alpha_e}{\alpha_e (1 - \alpha_e)} - \frac{f_2}{[1 + (a/b)] + \alpha_e} \right\} \right)^{-1}$$

The values of  $\alpha_e$  and  $a_e$  for the simplified air model are presented in figures A-1 and A-2 for temperatures up to 8000° K and for various pressure levels. The variations of  $a_f/a_e$  and  $\tau_r a_e$  are illustrated in figures A-3 and A-4. The maximum value of  $a_f/a_e$  for pure oxygen is roughly twice that for the air model. Pure oxygen, therefore, would have greater nonequilibrium effects than air, this being due to the lack of nitrogen acting as a diluent. The characteristic chemical reaction length for pure oxygen, on the other hand, is several times smaller than that for air because the nitrogen molecules are not as efficient a catalytic body for reaction as are oxygen molecules and atoms.

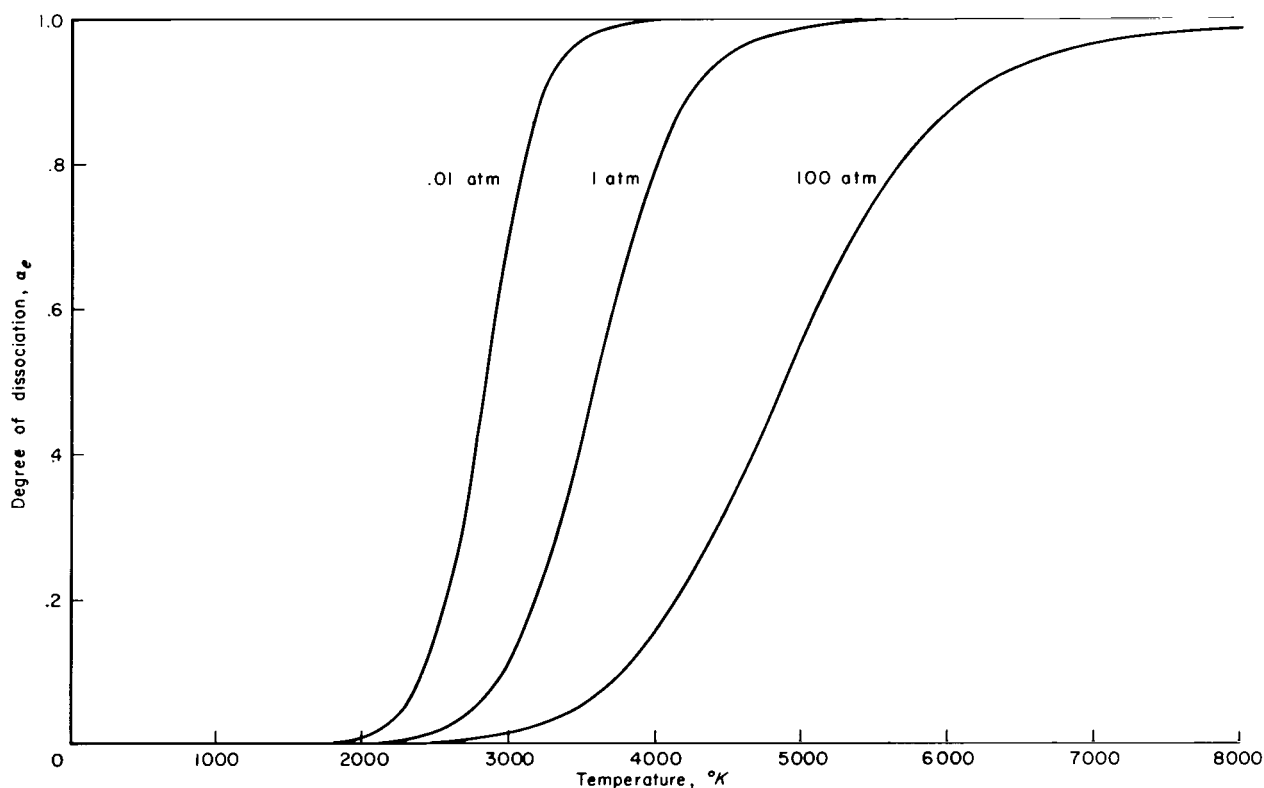


Figure A-1.- Equilibrium degree of dissociation versus temperature for pressure = 0.01, 1.0, and 100 atmospheres (simplified air model).

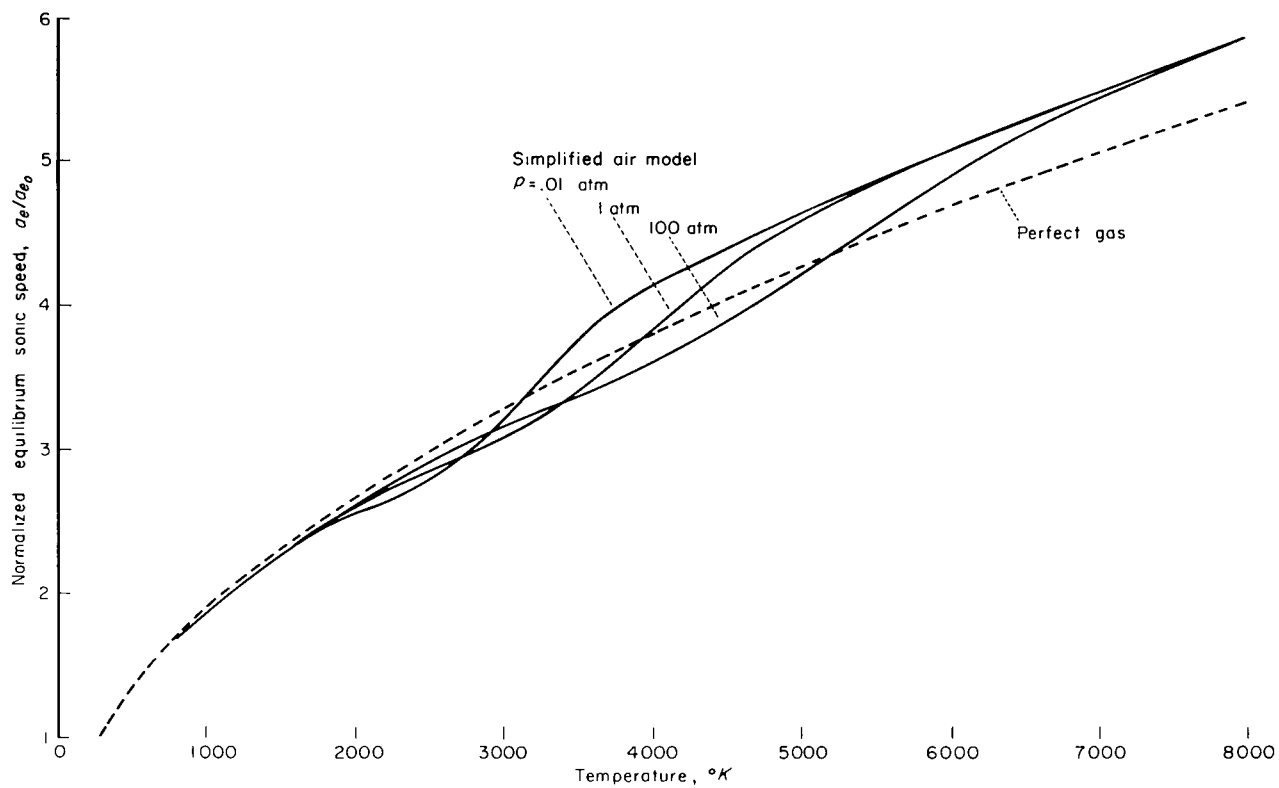


Figure A-2.- Equilibrium speed of sound versus temperature for pressure = 0.01, 1.0, and 100 atmospheres ( $a_{e0} = a_e$  at standard condition =  $3.320 \times 10^4$  cm/sec).

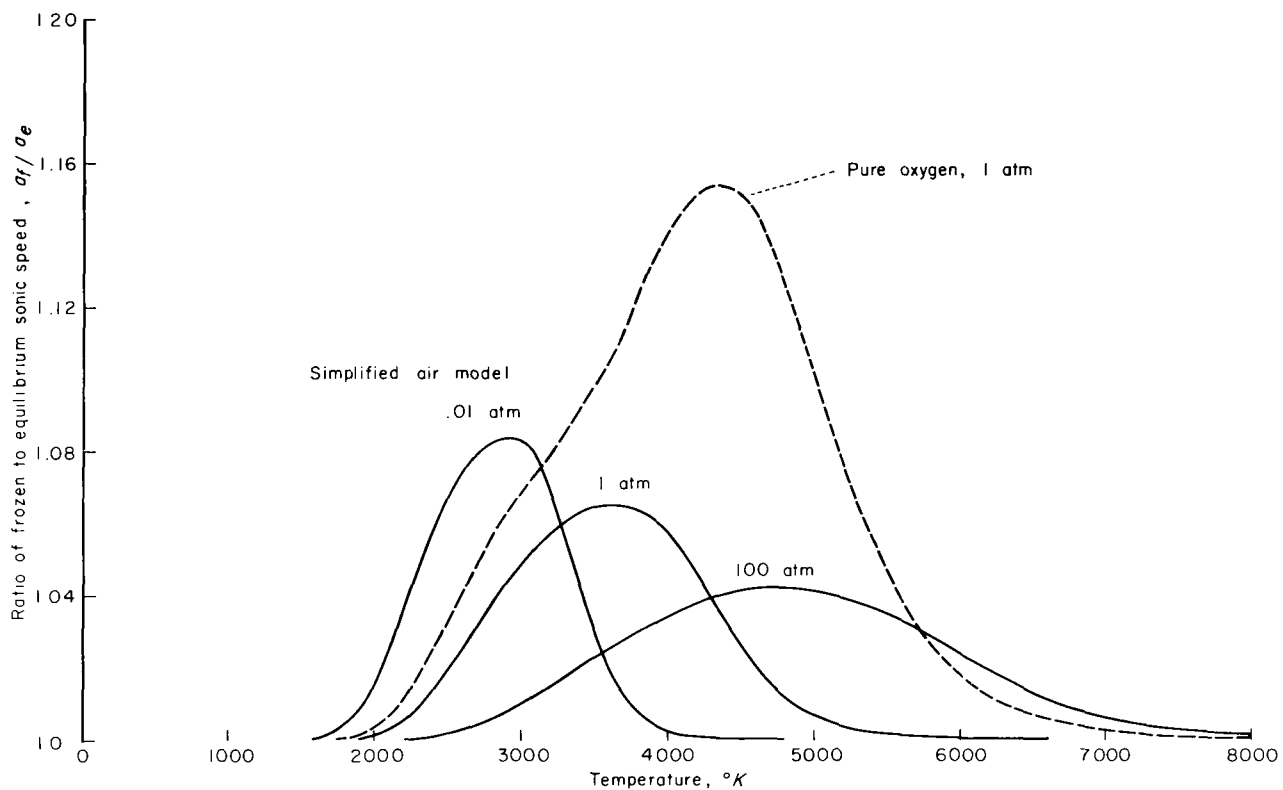


Figure A-3.- Ratio of frozen to equilibrium sonic speed for the simplified air model and for pure oxygen.

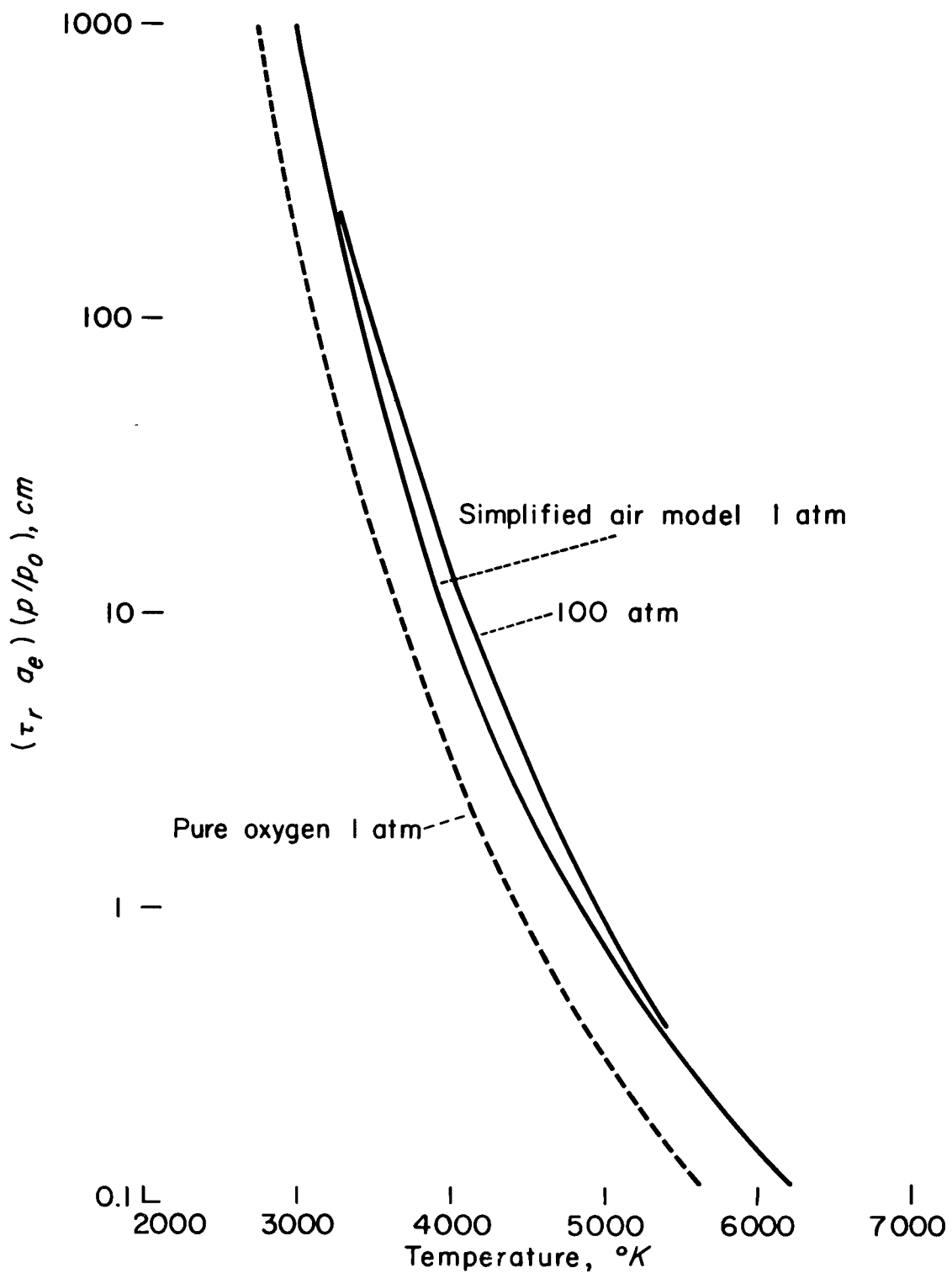


Figure A-4.- Normalized characteristic reaction length for the simplified air model and for pure oxygen.



TABLE I.- PHYSICAL CONSTANTS USED FOR THE GAS MODEL

a	3.3
b	0.8755
h	$6.6252 \times 10^{-27}$ erg sec
k	$1.38042 \times 10^{-16}$ erg/ $^{\circ}$ K
$m_0$	$2.66 \times 10^{-23}$
$M_0$	16 gm/mole
$\Theta_{D_{O_2}}$	59,380 $^{\circ}$ K
$\Theta_{D_{N_2}}$	113,260 $^{\circ}$ K
$\Theta_{r_{O_2}}$	2.07 $^{\circ}$ K
$\Theta_{v_{O_2}}$	2,230 $^{\circ}$ K
$\Theta_{v_{N_2}}$	3,340 $^{\circ}$ K

## APPENDIX B

### PRINCIPAL SYMBOLS

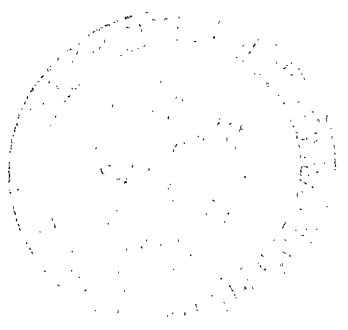
$a$	mass of oxygen/mass of nitrogen in gas model described in appendix A
$a_e$	equilibrium sonic speed
$a_f$	frozen sonic speed
$b$	ratio of atomic mass of nitrogen to atomic mass of oxygen
$e$	specific internal energy
$f$	any flow quantity or function
$h$	specific enthalpy; also Planck constant
$k$	Boltzmann constant
$k_f$	forward reaction rate constant
$K_c$	equilibrium constant
$m_O$	mass of an oxygen atom
$M$	Mach number (frozen or equilibrium)
$M_O$	atomic mass of oxygen
$n_i$	particle density of species $i$
$p$	pressure
$q$	nonequilibrium parameter
$q_i$	nonequilibrium parameter associated with the $i$ th process
$r$	radial distance from the axis of symmetry
$s$	streamwise distance
$S$	specific entropy
$t$	time
$T$	temperature

w	velocity
Z	compressibility factor; for the simplified air model, $1 + \alpha \left( 1 + \frac{a}{b} \right)^{-1}$
$\alpha$	degree of dissociation of oxygen = mass ratio of atomic oxygen to total amount of oxygen
$\beta$	$\sqrt{M^2 - 1}$
$\delta$	slope of the boundary
$\mu$	Mach angle = $\sin^{-1} \left( \frac{1}{M} \right)$
$\theta$	streamline angle
$\Theta_D, \Theta_r, \Theta_v$	characteristic temperatures for dissociation, rotation, and vibration, respectively
$\rho$	density of the fluid
$\tau_r$	characteristic reaction time (see eq. (A9))
$\omega$	rate of change of q

# REFERENCES

1. Bethe, H. A., and Teller, E.: Deviations from Thermal Equilibrium in Shock Waves. Rep. X-117, Aberdeen Proving Ground: Ballistic Res. Labs., 1945.
2. Ivey, H. Reese, and Cline, Charles W.: Effect of Heat-Capacity Lag on the Flow Through Oblique Shock Waves. NACA TN 2196, 1950.
3. Evans, John S.: Method for Calculating Effects of Dissociation on Flow Variables in the Relaxation Zone Behind Normal Shock Waves. NACA TN 3860, 1956.
4. Heims, Steve P.: Effect of Oxygen Recombination on One-Dimensional Flow at High Mach Numbers. NACA TN 4144, 1958.
5. Bray, K. N. C.: Atomic Recombination in a Hypersonic Wind-Tunnel Nozzle. Jour. Fluid Mech., vol. 6, pt. 1, July 1959, pp. 1-32.
6. Bray, K. N. C.: Simplified Sudden-Freezing Analysis for Nonequilibrium Nozzle Flows. ARS Jour., vol. 31, no. 6, June 1961, pp. 831-834.
7. Vincenti, Walter G.: Calculations of the One-Dimensional Nonequilibrium Flow of Air Through a Hypersonic Nozzle - Interim Report. SUDAER No. 101, Stanford Univ., Jan. 1961.
8. Emanuel, George, and Vincenti, Walter G.: Method for Calculation of the One-Dimensional Nonequilibrium Flow of a General Gas Mixture Through a Hypersonic Nozzle. Rep. AEDC-TDR-62-131, Arnold Eng. Dev. Center, June 1962.
9. Hall, J. Gordon, and Russo, Anthony L.: Studies of Chemical Nonequilibrium in Hypersonic Nozzle Flows. Rep. AD-1118-A-6, Cornell Aero Lab., Inc., Nov. 1959.
10. Eschenroeder, Alan Q., Boyer, Donald W., and Hall, J. Gordon: Exact Solutions for Nonequilibrium Expansions of Air with Coupled Chemical Reactions. Rep. AF-1413-A-1, Cornell Aero. Lab., Inc., May 1961.
11. Eschenroeder, Alan Q., Boyer, Donald W., and Hall, J. Gordon: Nonequilibrium Expansions of Air with Coupled Chemical Reactions. Phys. of Fluids, vol. 5, no. 5, May 1962, pp. 615-624.
12. Wood, William W., and Parker, F. R.: Structure of a Centered Rarefaction Wave in a Relaxing Gas. Phys. of Fluids, vol. 1, no. 3, May-June 1953, pp. 230-241.
13. Cleaver, J. W.: The Two-Dimensional Flow of an Ideal Dissociating Gas. Rep. 123, The College of Aeronautics, Cranfield, Dec. 1959.

14. Appleton, J. P.: The Structure of a Prandtl-Meyer Expansion Fan in an Ideal Dissociating Gas. U.S.A.A. Rep. 146, Univ. of Southampton, Aug. 1960.
15. Spence, D. A.: Unsteady Shock Propagation in a Relaxing Gas. Proc. Roy. Soc., A, vol. 264, no. 1317, Nov. 7, 1961, pp. 221-234.
16. Sedney, Raymond: Some Aspects of Non-Equilibrium Flows. Rep. 1099, Ballistic Res. Labs., Mar. 1960.
17. Lick, Wilbert: Inviscid Flow of a Reacting Mixture of Gases Around a Blunt Body. Jour. Fluid Mech., vol. 7, pt. 1, Jan. 1960, pp. 128-144.
18. Wood, William W., and Kirkwood, John G.: Hydrodynamics of a Reacting and Relaxing Fluid. Jour. Appl. Phys., vol. 28, no. 4, April 1957, pp. 395-398.
19. Chu, Boa-Teh: Wave Propagation and the Method of Characteristics in Reacting Gas Mixtures with Applications to Hypersonic Flow. WADC TN 57-213, May 1957.
20. Broer, L. J. F.: Characteristics of the Equations of Motion of a Reacting Gas. Jour. Fluid Mech., vol. 4, pt. 3, July 1958, pp. 276-282.
21. Der, James J.: Linearized Supersonic Nonequilibrium Flow Past an Arbitrary Boundary. NASA TR R-119, 1961.
22. Vincenti, Walter G.: Lectures on Physical Gas Dynamics. Stanford Univ., 1961.
23. Courant, R.: Partial Differential Equations. Vol. II of Methods of Mathematical Physics. Interscience Publishers, 1962.
24. von Mises, Richard (completed by Hilda Geiringer and G. S. S. Ludford): Mathematical Theory of Compressible Fluid Flow. Academic Press, Inc., 1958.
25. Lighthill, M. J.: Dynamics of a Dissociating Gas. Part I: Equilibrium Flow. Jour. Fluid Mech., vol. 2, pt. 1, Jan. 1957, pp. 1-32.
26. Freeman, N. C.: Non-Equilibrium Flow of an Ideal Dissociating Gas. Jour. Fluid Mech., vol. 4, pt. 4, Aug. 1958, pp. 407-425.
27. Yoshikawa, Kenneth K., and Katzen, Elliott D.: Charts for Air-Flow Properties in Equilibrium and Frozen Flows in Hypervelocity Nozzles. NASA TN D-693, 1961.
28. Hinshelwood, C. N.: The Kinetics of Chemical Change. Oxford Univ. Press (London), 1940.
29. Rushbrooke, G. S.: Introduction to Statistical Mechanics. Oxford Univ. Press (London), 1949.



*"The aeronautical and space activities of the United States shall be conducted so as to contribute . . . to the expansion of human knowledge of phenomena in the atmosphere and space. The Administration shall provide for the widest practicable and appropriate dissemination of information concerning its activities and the results thereof."*

—NATIONAL AERONAUTICS AND SPACE ACT OF 1958

## NASA SCIENTIFIC AND TECHNICAL PUBLICATIONS

**TECHNICAL REPORTS:** Scientific and technical information considered important, complete, and a lasting contribution to existing knowledge.

**TECHNICAL NOTES:** Information less broad in scope but nevertheless of importance as a contribution to existing knowledge.

**TECHNICAL MEMORANDUMS:** Information receiving limited distribution because of preliminary data, security classification, or other reasons.

**CONTRACTOR REPORTS:** Technical information generated in connection with a NASA contract or grant and released under NASA auspices.

**TECHNICAL TRANSLATIONS:** Information published in a foreign language considered to merit NASA distribution in English.

**TECHNICAL REPRINTS:** Information derived from NASA activities and initially published in the form of journal articles.

**SPECIAL PUBLICATIONS:** Information derived from or of value to NASA activities but not necessarily reporting the results of individual NASA-programmed scientific efforts. Publications include conference proceedings, monographs, data compilations, handbooks, sourcebooks, and special bibliographies.

*Details on the availability of these publications may be obtained from:*

SCIENTIFIC AND TECHNICAL INFORMATION DIVISION  
NATIONAL AERONAUTICS AND SPACE ADMINISTRATION

Washington, D.C. 20546